PHYSICS EDUCATION

INDIAN ASSOCIATION OF PHYSICS TEACHERS

IAPT

Serge Haroche   David J. Wineland

The Nobel Prize Winners in Physics 2012

www.physedu.in

Volume 28, Number 4

In this Issue

EDITORIAL

(*Submitted Dec 2012*)

We come to the end of the first year of the operation of the online version of Physics Education. I am afraid we did encounter a few bugs in the editorial processing and we are happy that we have fixed most of them. This has also been a valuable learning experience for the Physics Education team and look forward to a better process for the next volume.

The policy for Physics Education is governed by the motto swift and fair editorial processing. For this to happen we need an active involvement of all our editors and the referees who assist them in this process. I would like to suggest that the editors initiate the process within a week of the receipt of the manuscript and the referees respond within reasonable time. The authors are also asked to respond to the referee's suggestions/comments, so that their contribution is more useful for the readers.

We look forward to the journal serving the needs of the pedagogy by sharing of the experiences of the teachers in their class room. We encourage our authors to submit contributions that could be used in our sequences such as Physics through teaching lab, Physics through problem solving and Physics through computations and simulations.

Pramod S. Joag.
Chief-editor@physedu.in,
pramod@physics.unipune.ac.in
Chief Editor

R Ramchandran
rr_1940@yahoo.co.in
Consulting Editor

An extension of the particle in a one dimensional box model

Cristiano C. Bastos[1], Gerson S. Paiva[2], Eduardo S. G. Leandro[3], and Antonio C. Pavão[1]

[1]Departamento de Química Fundamental
Universidade Federal de Pernambuco
Recife 50670-901, Brazil.

[2]Centro Brasileiro de Pesquisas Físicas
Rio de Janeiro 22290-180, Brazil

[3]Departamento de Matemática
Universidade Federal de Pernambuco
Recife 50740-540, Brazil

Abstract

Under the hypotheses commonly employed in textbooks, we calculated the spectrum of a particle in a one-dimensional regular curve embedded in 2D with a general smooth parameterization x = g(t) and y = h(t), where t is the curve parameter. The solution of the one-dimensional Schrödinger equation under the confined boundary conditions corresponding to our generalized particle in a box model shows that the linear box has the same energy spectrum as parabolas, cubics, exponentials, or any other open regular curves: $E = h^2n^2/8mL^2$, whereas the circular box has the same energy spectrum as ellipses, ovals, or any other closed regular curves: $E = h^2n^2/2mL^2$. There are many studies of quantum mechanics on curves using different theoretical approaches, however the present elementary approach and its conclusions are not found in the literature. We observe that the Schrödinger equation does not make sense when applied to spaces that are not manifolds.

1. The particle in a box problem

The particle in a box model (PIB model) is one of the most fundamental and versatile tools in the history of quantum mechanics [1-5]. Since Erwin Schrödinger's pioneering paper published in 1926 [1], the PIB model has emerged in a number of studies on diverse subjects such as: the spectrum of solids, the electronic absorption spectrum, nuclei, specific heat, optical rotation, NMR, PIB in the presence of an electric field, and the particle in a ring system. But the PIB model *is not so simple*, as evidenced by its applications in quantum mechanics propagators, Feynman path integrals, quark confinement and the Casimir effect, delta potential, two particles in two boxes, minimum Planck length, the PIB relativistic model, D-dimensional PIB, and quantum dots in nanotechnology [3-13]. In light of these different approaches, it is worth asking: how is the energy spectrum of the particle modified as a result of changes in the geometry of the curve? The answer to this question, that we were not able to find in the

chemistry and physics literatures [9-15], could help to further expand the applicability of the PIB model. Let us start with the circular box problem (rotator with fixed axis), which was first solved by Schrödinger [1] using the eigenvalue equation:

$$H\Psi(\phi) = -\frac{\hbar^2}{2mr^2}\frac{d^2}{d\phi^2}\Psi(\phi) = E\Psi(\phi) \qquad (1)$$

where m is the rest-mass of the particle and r is the circumference radius. Using the boundary condition for the wave function $\Psi(\phi) = \Psi(\phi+2\pi)$, the particle energy is $E = (h^2n^2/2mL^2)$, where $L = 2\pi r$ is the length of the one-dimensional box [1,5,6]. The PIB model has since spread to classrooms and textbooks, and it has been revisited, directly or indirectly, in scientific and didactic papers [1-13]. As a result, the PIB model is now considered one of the fundamental problems in quantum mechanics. In this paper, we provide an extended PIB model taking into account a box with a smooth shape in order to calculate the spectrum of a particle in any one-dimensional regular curve embedded in 2D. We found two expressions for the energy spectrum: $E = h^2n^2/8mL^2$ for open curves and $E = h^2n^2/2mL^2$ for closed curves. This means that, once fixed the length, the linear box has the same energy spectrum as parabolas, cubics, exponentials or any other open regular curves. Also, the circular box has the same energy spectrum as ellipses, ovals, or any other closed regular curves possessing the same length.

2. The one-dimensional Laplacian operator

Let us consider the following parametrization of a smooth regular curve $x = g(t)$ and $y = h(t)$, where t is the parameter (t is not the time).
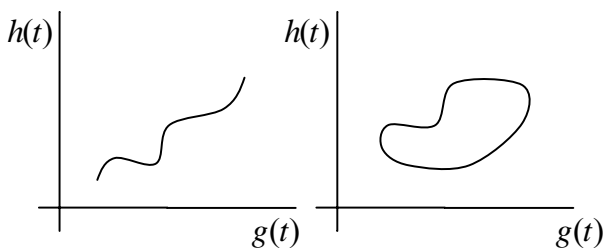

Figure 1. Open and closed regular curves.

We recall that a smooth curve is said to be regular if its velocity vector, $\alpha`(t) = (g`(t), h`(t))$, is nowhere vanishing. Taking into account this parameterization, we obtain the one-dimensional Laplacian operator (Laplace-Beltrami) on the curve and rewrite it in the arc-length variable s:

$$\nabla^2 = g^{-1/2}\frac{\partial}{\partial q^i}\left(g^{1/2}g^{ik}\frac{\partial}{\partial q^k}\right) = g^{-1/2}\frac{d}{dt}\left(g^{-1/2}\frac{d}{dt}\right).$$

Since:

$$g^{1/2} = g_{11}{}^{1/2} = \sqrt{\left(\frac{dx}{dt}\right)^2 + \left(\frac{dy}{dt}\right)^2} = \frac{ds}{dt},$$

it follows that:

$$\nabla^2 = \frac{d^2}{ds^2}. \qquad (2)$$

Using expression 2., note that in the original case of equation 1. (using t as angle) we have $x = r\cos t$ and $y = r\sin t$ and find the Laplacian operator $\nabla^2 = d^2/dx^2 + d^2/dy^2 = (1/r^2)d^2/dt^2$ (the arc length depends on the angle and the radius).
Using the Laplacian operator 2., the Schrödinger equation 1. turns out to be in the well known case:

$$\frac{d^2}{ds^2}\Psi(s) = -\frac{2mE}{\hbar^2}\Psi(s) \qquad (3)$$

This is the usual one-dimensional harmonic oscillator equation, and from this point on the discussion of eigenvalues and eigenfunction follows the traditional steps. We can now solve the PIB model by using equation 3. and considering the two possible cases of boundary conditions. For the open curve (linear or not), the boundary conditions are $\Psi(s_o) = \Psi(s_1) = 0$, which are similar to those of the linear box [4]; for the closed curve, the boundary conditions are $\Psi(s_o) = \Psi(s_1)$ (univalued periodic wave function condition), which are similar to those of the circular box [1].
The general solution of 3. is $\Psi(s) = A\sin(ks) + B\cos(ks)$, with A and B real constants. The parameter k relates to the energy as follows:

$$k^2 = \frac{2mE}{\hbar^2}$$

The arc length relates to the box length L as indicated by the equation:

$$L = \int_{t_o}^{t_1} \sqrt{\left(\frac{dx}{dt}\right)^2 + \left(\frac{dy}{dt}\right)^2}\, dt = s(t_1) - s(t_o) \equiv s_1 - s_o$$

Using this result for the open curve, with the usual assumption $s_o = 0$, and the boundary condition requires $\Psi(s_o) = \Psi(s_1) = 0$, then $A\sin(ks_o) = A\sin(ks_1) = 0$, $ks_o = m\pi$ and, from the periodicity of the sine function, $ks_1 = m\pi + n\pi$, $ks_1 - ks_o = k(s_1 - s_o) = kL = n\pi$, where n is a natural number. In order to find a final expression for the energy, we have:

$$k^2 = \frac{2mE}{\hbar^2} = \frac{n^2\pi^2}{L^2}$$

$$E = \frac{h^2 n^2}{8mL^2} \qquad (4)$$

This relation describes the energy spectrum of any regular open curve, such as straight lines, parabolas, hyperbolas, cubics, sinusoidal curves, etc.

For a closed curve, let s_o be the initial arc length and let s_1 be the arc length after one turn around the curve $L = s_1 - s_o$. In order to find an expression for the energy, we impose the boundary condition $\Psi(s_o) = A\sin(ks_o) + B\cos(ks_o) = \Psi(s_1) = A\sin(ks_1) + B\cos(ks_1)$ and the periodicity condition $\Psi(s_o) = \Psi(s_o + L)$; from the periodicity of the sine function, $ks_1 = ks_o + (2\pi n)$, then $k = (2\pi n)/L$, where n is an integer number, we deduce:

$$k^2 = \frac{2mE}{\hbar^2} = \frac{4\pi^2 n^2}{L^2}$$

$$E = \frac{h^2 n^2}{2mL^2} \qquad (5)$$

Relation 5. describes the energy spectrum for the conventional circular box with length L, and, as evidenced above, it actually describes the energy spectrum of any regular closed curve, for example ellipses, ovals, smoothed polygons, etc. The two expressions 4. and 5. show that, for regular curves of the same length L, the energy spectrum can be used to distinguish between open and closed curves. For the same n, we have $E_{closed} = 4E_{open}$. As far as we know, this result is not found in the literature [1-13]. It represents an explicit general solution for the PIB model of regular curves under the usual hypotheses found in textbooks [2, 9-12].

3. Mathematical note

It is well known in differential topology [16] that a smooth curve which is a manifold (locally, at each point, it looks like a line segment) can only be diffeomorphic to either a line segment or a circle. In this paper, we show that the energy spectrum of a smooth, regular curve of a fixed length is determined by this topological classification; the topology (open or closed) of such a curve, whose length is known, suffices to determine its spectrum, and conversely, given the length of the curve, the energy spectrum determines the topology of the curve. Although this is a criterion which mixes topology and geometry, a purely topological criterion can be obtained by noticing that, for all closed regular curves, the eigenfunctions come in pairs, sine and cosine, and zero is also an admissible eigenvalue. These properties are not shared by open regular curves.

The problem of understanding the topology of a manifold from its spectrum is currently of interest in Mathematics. In that sense, a classical reference to this problem is the famous paper "Can you hear the shape of a drum?" by Mark Kac [17]. In this paper, we show that you can "hear the topology" of a 1D drum, provided you know its length. Notice that smooth curves with self-intersections are not manifolds in general and thus cannot be treated in the same way as regular embedded curves. The Schrödinger equation actually does not make sense when applied to spaces that are not manifolds since the Laplacian is no longer globally defined.

4. Conclusions

We used the corresponding Laplacian operator for a smooth curve with a general parameterization in the Schrödinger equation and found the eigenfunctions $\Psi(s) = A\sin(ks) + B\cos(ks)$, where s is the arc length parameter, and energy spectrum E given by only two possible expressions: $E = h^2n^2/8mL^2$ for open curves, and $E = h^2n^2/2mL^2$ for closed curves. This result is a new contribution to the literature on the PIB model spectrum calculation of a particle constrained to a one-dimensional regular curve embedded in a 2D surface.

Acknowledgements

References:

[1] E. Schrödinger, Ann. Phys. **79**, 13 (1926).
[2] L. Pauling, *Introduction to Quantum Mechanics*, (Mc Graw-Hill, New York, 1935).
[3] F. E. Cummings, Am. J. Phys. **45**, 158 (1977).
[4] K. Volkamer and M. J. Lerom, J. Chem. Educ. **69**, 100 (1992).
[5] A. J. Vicent, J. Chem Educ. **73**, 1001 (1996).
[6] N. Bera, J. Bhattacharjee, S. Mitra and S. Khastgir, Eur. Phys. J. D **46**,41 (2008).
[7] W. Li and S. Blinder, Chem. Phys. Lett. **496**, 339 (2010).
[8] J. Gravesen and M. Willatzen, Physica B **371**, 112 (2006).
[9] C. Cohen-Tanoudji, B. Diu, F. Laloë, *Quantum Mechanics*, (John Wiley & Sons, New York, 2005).
[10] S. Gasiorowicz, *Quantum Physics*, (John Wiley & Sons, Inc., 1974).
[11] J. Griffits, *Introduction to Quantum Mechanics*, (Pearson Prentice Hall, 2005).
[12] P. W. Atkins and R. Friedman. *Molecular Quantum Mechanics*, (Oxford University Press Inc., New York, 2005).
[13] E. Miliordos, Phys. Rev. A **82**, 062118-1 (2010).
[14] R. Froese and I. Herbst, Israel J. Math. **170**, 337 (2009).
[15] E. M. Harrell II and M. Loss, Math. Phys. **195**, 643 (1998).
[16] J. Milnor, *Topology from the Differential Viewpoint*, (Princeton University Press, Princeton, NJ, 1965).
[17] M. Kac, Am. Math. Monthly, **73**, 1 (1966).

Who is Afraid of Special Functions and Orthogonal Polynomials in Quantum Mechanics

Abhijit Sen[a,1]*, N. Gurappa[b,2], Rajneesh Atre [c,3] and Prasanta K. Panigrahi[a,4]

[1]abhijisen@yahoo.co.in; [2]dr.n.gurappa@gmail.com;
[3]darvish.rajneesh@gmail.com; [4]pprasanta@iiserkol.ac.in

[a]Indian Institute of Science Education and Research-Kolkata,
Mohanpur, Nadia-741252, West Bengal, India

[b]Priyadarshini College of Engineering,
Sullurpet-524121, Andhra Pradesh,

[c]Department of Physics,
Jaypee Institute of Engineering and Technology,
Guna-473226, India

(Submitted Apr 2012)

Abstract

We explicate a novel procedure to solve general linear differential equations, which routinely manifest in Quantum Mechanics. These equations include Hermite, Laguerre, Jocobi, Bessel and hypergeometric etc. The present approach connects the desired solutions to monomials x^λ, of an appropriate degree λ. In the process the underlying symmetry of the equations under study, as well as that of the solutions are made transparent. We demonstrate the efficacy of the method by showing the common structure of the solution space of a wide variety of differential equations. We also illustrate the use of the procedure to develop approximate solutions through the examples of sextic and anharmonic oscillators. We further use the method in finding solutions of many particle interacting systems through the examples of Calogero-Sutherland and Sutherland type of models.

1 Introduction

Well-known classical orthogonal polynomials and functions like Bessel, Airy etc., manifest as solutions of Schrodinger equation in quantum mechanics, in the study of waves, in optics and electromagnetism. As is evident, the basic building blocks of polynomials and functions are the monomials. Superposition of finite and infinite number of these constituents, with appropriate coefficients, respectively leads to various polynomials and functions.

Apart from finding solutions of various differential equations, considerable effort has been put into understanding the symmetry properties of these equations, which throw light on the structure of the solution space [1]. Here, we illustrate a procedure of solving linear differential equations, which leads to an exact mapping between the desired polynomials and functions and the space of monomials [2, 3]. In this method, the Euler operator (EO) $D \equiv x\frac{d}{dx}$ plays a crucial role. It makes essential use of the two properties of the EO.

1. The monomials are the eigenfunctions of the EO:

$$x\frac{d}{dx}x^\lambda \equiv Dx^\lambda = \lambda x^\lambda, \qquad (1)$$

2. The Euler operator 'measures' the degree of an operator, irrespective of its constituents,

$$[D, O^d] = dO^d, \qquad (2)$$

---

on leave of absence from Suri Vidyasagar College, Suri, West Bengal-731101, India,

where O^d is an operator of 'degree' d e.g., x^2 and $x^3\frac{d}{dx}$ have degree 2, while $\frac{d^2}{dx^2}$ and $\frac{d^2}{dx^2} + \frac{\alpha}{x^2}$ have degree -2.

In the space of monomials Eq.(1) shows that the eigenvalues of the Euler operator are all real. Upon acting on a monomial x^n, it behaves like an eigenvalue equation as depicted in Eq.(2), 'bringing down' the exponent as the eigenvalue. This property of the Euler operator is key to the present technique of solving differential equations, as shall be soon evident.

In the following, we start with the familiar Hermite, Laguerre and confluent hypergeometric equations and make use of their symmetry properties to obtain solutions in a form, which exhibits the mapping between the respective polynomials and the space of monomials. We then explicate a more general method, applicable to linear differential equations of arbitrary order and obtain the desired solutions making use of the above mentioned properties of the Euler operator. The procedure is explicated through solution of the oscillator problem. Subsequently, earlier solved examples are connected with the new approach, considering Hermite differential equation as the example. After illustrating the solution space of the hypergeometric equation, we tabulate the solutions and the structure of their respective differential equations for all the functions and polynomials, commonly encountered in physics literature. The case of the so called quasi-exactly solvable Schrodinger equation is then studied, for which only a part of the spectrum is analytically obtainable. This example also shows the use of the present approach for finding

---

the exact solution, as well as in the development of approximation schemes. We then proceed to many-body interacting Calogero- Sutherland systems and show how our procedure can be profitably utilized for finding out the eigenspectra and eigenfunctions. We conclude with directions for future work.

2   Connecting Polynomials with Monomials

We start with the well studied Hermite differential equation:

$$[-\frac{1}{2}\frac{d^2}{dx^2} + (D-n)]H_n(x) \equiv \hat{O}H_n(x) = 0, \tag{3}$$

which has seen the use of traditional series solution method to the algebraic approach of raising and lowering operators, for finding the solution [4]. It is worthwhile to observe that the above equation has the Euler operator and a degree d=-2 operator $-\frac{1}{2}\frac{d^2}{dx^2} = P$, apart from a harmless constant. The fact that $[D, P] = -2P$ can be profitably used through the Baker-Campbell-Hausdorff (BCH) formula:

$$e^A B e^{-A} = B + [A, B] + \frac{1}{2}[A, [A, B]] + ..., \tag{4}$$

in order to map the differential operator $\hat{O}$ onto (D-n).
For this purpose, it can be checked that (Refer to Appendix I for a proof),

$$e^{\frac{1}{4}\frac{d^2}{dx^2}}[-\frac{1}{2}\frac{d^2}{dx^2} + D - n]e^{-\frac{1}{4}\frac{d^2}{dx^2}} = -\frac{1}{2}\frac{d^2}{dx^2} + D - n + \frac{1}{4}[\frac{d^2}{dx^2}, D] = (D-n). \tag{5}$$

This immidiately suggests to factorize the Hermite polynomial in the form

$$[-\frac{1}{2}\frac{d^2}{dx^2} + D - n]e^{-\frac{1}{4}\frac{d^2}{dx^2}}\varphi(x) = e^{-\frac{1}{4}\frac{d^2}{dx^2}}[D-n]\varphi(x) = 0, \tag{6}$$

which implies,

$$[D - n]\varphi(x) = 0. \tag{7}$$

The fact that the monomials are eigenfunctions of the Euler operator D leads to $\phi(x) = c_n x^n$ and hence the Hermite polynomial becomes, $H_n(x) = c_n e^{-\frac{1}{4}\frac{d^2}{dx^2}} x^n$. The above is the exact connection between the monomial x^n and the polynomial $H_n(x)$; the value of c_n is to be

determined from normalization condition. The discerning reader can visualize that the structure of Laguerre differential equation,

$$[x\frac{d}{dx} - n - (\alpha + 1)\frac{d}{dx} - x\frac{d^2}{dx^2}]L_n^\alpha(x) = 0, \tag{8}$$

and confluent hypergeometric equation,

$$[x\frac{d}{dx} + \alpha - x\frac{d^2}{dx^2} - \gamma\frac{d}{dx}]\Phi(\alpha, \gamma, x) = 0, \tag{9}$$

are similar to the Hermite case. A similar mapping connects the above differential operators to $(D-n)$ and hence the solutions can be written in the form, $L_n^\alpha = c_n exp[-x\frac{d^2}{dx^2} - (\alpha+1)\frac{d}{dx}]x^n$ [5] and $\Phi(\alpha, \gamma, x) = c_{-\alpha}exp[-x\frac{d^2}{dx^2} - \gamma\frac{d}{dx}]x^{-\alpha}$.

This procedure can be used to identify the generating function and the algebraic structure of the solution space [6]. We refer the interested reader to Ref.[2] for more details, as also to Ref.[7], for construction of coherent states for the dynamical systems, associated with the harmonic oscillator and other quantal problems.

It is evident that, if the differential operator $\hat{O}$ contains an operator of definite degree, apart from the Euler operator and the constant term, the aforementioned approach can connect the solution space to monomials through an exponential mapping. It may not be the case in general. Keeping this in mind, in the next section we develop a more general approach connecting the solution space with monomials for general equations.

3 A Simple Approach to Familiar Differential Equations: Alternate Representations for Special Functions

For simplicity, we will first consider the case of single variable linear differential equations (LDEs) and deal with its multi-variate generalization later. A single variable LDE, as will become clear from the examples of later sections, can be cast in the form

$$[F(D) + P(x, d/dx)]\, y(x) = 0, \tag{10}$$

where, $F(D) \equiv \sum_{n=-\infty}^{n=\infty} a_n D^n$ and a_n's are some parameters; $P(x, d/dx)$ can be an arbitrary polynomial function of $x, d/dx$ and other operators. The solution to Eq.(10) can be written as [2],

$$y(x) = C_\lambda \left\{ \sum_{m=0}^{\infty} (-1)^m \left[\frac{1}{F(D)} P(x, d/dx) \right]^m \right\} x^\lambda, \tag{11}$$

provided, $F(D)x^\lambda = 0$; here C_λ is constant. It is easy to see that, the operator $1/F(D)$ is well defined in the above expression and will not lead to any singularity, if $P(x, d/dx)$ does not contain any degree zero operator. We note that D itself is an operator of degree zero.

The proof of Eq.(11) follows by direct substitution [3]. Please refer to Appendix-II for details,

Since $F(D)x^\lambda = 0$, equating $F(D)x^\lambda$ modulo C_λ and Eq. (10), one finds,

$$[F(D) + P(x, d/dx)] \, y(x) = C_\lambda F(D)x^\lambda. \tag{12}$$

Rearranging the above equation in the form

$$F(D) \left[1 + \frac{1}{F(D)} P(x, d/dx)\right] y(x) = C_\lambda F(D)x^\lambda, \tag{13}$$

and cancelling $F(D)$, we obtain

$$\left[1 + \frac{1}{F(D)} P(x, d/dx)\right] y(x) = C_\lambda x^\lambda. \tag{14}$$

This yields

$$y(x) = C_\lambda \frac{1}{\left[1 + \frac{1}{F(D)} P(x, d/dx)\right]} x^\lambda, \tag{15}$$

which can be cast in the desired series form:

$$y(x) = C_\lambda \left\{ \sum_{m=0}^{\infty} (-1)^m \left[\frac{1}{F(D)} P(x, d/dx)\right]^m \right\} x^\lambda. \tag{16}$$

It is explicit that, the above procedure connects the solution $y(x)$ to the space of the monomials x^λ. The generalization of this method to a wide class of many-variable problems is immediate. Using the fact that, $F(\bar{D})X^\lambda = 0$ has solutions, in the space of monomial symmetric functions [8], where $\bar{D} = \sum_i D_i \equiv \sum_i x_i \frac{d}{dx_i}$, the solutions of those multi-variate DEs, which can be separated into the form given in Eq.(10), can be obtained like the single variable case. As will be seen later, this procedure enables one to solve a number of many-body problems. We shall consider such systems shortly.

For illustration, we consider the harmonic oscillator problem. The Schrodinger eigenvalue equation (in the units, $\hbar = \omega = m = 1$),

$$\left[\frac{d^2}{dx^2} + (2E_n - x^2)\right] \psi_n = 0, \tag{17}$$

can be written in the form given in Eq.(10), after multiplying it by x^2 :

$$\left[(D-1)D + x^2(2E_n - x^2)\right]\psi_n = 0. \tag{18}$$

Here, $F(D) = (D-1)D$ and the condition $F(D)x^\lambda = 0$ yields, $\lambda = 0$ or 1. Using Eq.(11), the solution for $\lambda = 0$ is,

$$\begin{aligned}
\psi_0 &= C_0\left\{\sum_{m=0}^{\infty}(-1)^m\left[\frac{1}{(D-1)D}(x^2(2E_0 - x^2))\right]^m\right\}x^0 \\
&= C_0\left[1 - \frac{[2E_0]}{2!}x^2 + \frac{(2! + [2E_0]^2)}{4!}x^4 - \frac{(4! + (2!)^2[2E_0] + (2!)[2E_0]^3)}{2!6!}x^6 + \cdots\right] \tag{19}
\end{aligned}$$

It is worth noting that in Quantum Mechanics, a function is square integrable if as square integrable, if the integral of the square of the absolute value of the function (i.e., $|f(x)|^2$) is finite upon integrating over all space ($-\infty$ to ∞ for functions in one space dimension). This condition is referred to as square integrability condition. Here ψ_0 is an expansion in powers of x, whose coefficients are polynomials in E_0. The above series can be written in a closed, square integrable form, $C_0\exp(-x^2/2)$, only when $E_0 = 1/2$. Analogously, $\lambda = 1$, yields the first excited state. To find the nth excited state, one has to differentiate the Schrodinger equation $(n-2)$ number of times and subsequently multiply it by x^n to produce $F(D) = x^n\frac{d^n}{dx^n} = \prod_{l=0}^{n-1}(D-l)$, and proceed in a manner similar to the ground state case.

It is clear that, our procedure yields a series solution, where additional conditions like square integrability has to be imposed to obtain physical eigenfunctions and their corresponding eigenvalues. Once, the ground state has been identified and for those cases, where $\psi(x) = \psi_0 P(x)$, where $P(x)$ is a polynomial, one can effortlessly obtain the polynomial part, as will be shown below.

Returning to the harmonic oscillator case and writing for ψ_n as

$$\psi_\alpha(x) = e^{-x^2/2}H_\alpha(x), \tag{20}$$

one can easily show that H_α satisfies,

$$\left[D - \alpha - \frac{1}{2}\frac{d^2}{dx^2}\right]H_\alpha(x) = 0, \tag{21}$$

where $\alpha = E_n - 1/2$. The solution of the DE is given by

$$H_\alpha(x) = C_\alpha\sum_{m=0}^{\infty}(-1)^m\left[-\frac{1}{D-\alpha}\frac{1}{2}\frac{d^2}{dx^2}\right]^m x^\alpha, \tag{22}$$

which yields a polynomial, only when α is an integer, since the operator d^2/dx^2 reduces the degree of x^α by two, in each step. Setting $\alpha = n$ in Eq.(21), we obtain the Hermite DE and $E_n = (n + 1/2)$ as the energy eigenvalue. Below, we give the algebraic manipulations required to cast the series solution of Eq.(22) into a form, not very familiar in the literature. For the Hermite DE, $F(D) = D - n$ and $P(x, d/dx) = -\frac{1}{2}\frac{d^2}{dx^2}$, the condition $F(D)x^\lambda = 0$ yields $\lambda = n$, hence,

$$H_n(x) = C_n \sum_{m=0}^{\infty} (-1)^m \left[-\frac{1}{(D-n)}\frac{1}{2}\frac{d^2}{dx^2} \right]^m x^n. \tag{23}$$

Using, $[D, (d^2/dx^2)] = -2(d^2/dx^2)$ and making use of the fact

$$\frac{1}{D-n} = \int_0^\infty ds\, e^{-s(D-n)} \tag{24}$$

we can write,

$$\left[-\frac{1}{2}\frac{1}{(D-n)}\frac{d^2}{dx^2} \right] = -\frac{1}{2}\frac{d^2}{dx^2}\frac{1}{(D-n-2)},$$

$$\left[-\frac{1}{2}\frac{1}{(D-n)}\frac{d^2}{dx^2} \right]\left[-\frac{1}{2}\frac{1}{(D-n)}\frac{d^2}{dx^2} \right] = \left[-\frac{1}{2}\frac{d^2}{dx^2} \right]^2 \frac{1}{(D-n-4)}\frac{1}{(D-n-2)}. \tag{25}$$

Hence in general,

$$\left[-\frac{1}{2}\frac{1}{(D-n)}\frac{d^2}{dx^2} \right]^m x^n = \left(-\frac{1}{2}\frac{d^2}{dx^2} \right)^m \prod_{l=1}^{m} \frac{1}{(-2l)} x^n$$

$$= \frac{1}{m!}\left(\frac{1}{4}\frac{d^2}{dx^2} \right)^m x^n. \tag{26}$$

Substituting Eq.(26) in Eq.(23), we obtain,

$$H_n(x) = C_n \sum_{m=0}^{\infty} (-1)^m \frac{1}{m!}\left(\frac{1}{4}\frac{d^2}{dx^2} \right)^m x^n$$

$$= C_n \exp\left(-\frac{1}{4}\frac{d^2}{dx^2} \right) x^n, \tag{27}$$

a result, not commonly found in the literature. The arbitrary constant C_n is chosen to be 2^n, so that the polynomials obtained can match with the standard definition [9].

Likewise, the solution to the hypergeometric DE,

$$\left[x^2 \frac{d^2}{dx^2} + (\alpha + \beta + 1)\, x \frac{d}{dx} + \alpha\beta - x \frac{d^2}{dx^2} - \gamma \frac{d}{dx} \right] F(\alpha, \beta; \gamma; x) = 0 \qquad (28)$$

can be written as,

$$F(\alpha, \beta; \gamma; x) = (-1)^{-\beta} \frac{\Gamma(\alpha - \beta)\Gamma(\gamma)}{\Gamma(\gamma - \beta)\Gamma(\alpha)} \exp\left[\frac{-1}{(D + \alpha)} \left(x \frac{d^2}{dx^2} + \gamma \frac{d}{dx} \right) \right] x^{-\beta}. \qquad (29)$$

For convenience a table has been provided at the end, which lists a number of commonly encountered DEs and the novel exponential forms of their solutions. It is worth pointing out that, the solution of hypergeometric DE is a polynomial solution, provided either α or β is a negative integer. It should be noticed that, unlike the conventional expressions, the monomials in the above solutions are arranged in decreasing powers of x.

Multiplying the hypergeometric DE with x yields two roots, $\lambda = 0, 1 - \gamma$ and $\lambda = 0$ solution gives rise to the well-known, Gauss hypergeometric series. Since a number of quantum mechanical problems can be related to confluent and hypergeometric DEs [10], we hope that, the novel expressions given above and in the table, will find physical applications.

4 Quasi-Exactly Solvable Problems: Sextic and Anharmonic Oscillators

This section is devoted to the study of QES problems [11]. These problems are intermediate to exactly and non-exactly solvable quantum potentials, in the sense that, only a part of the spectrum can be determined analytically. These potentials have attracted considerable attention in recent times, because of their connection to various physical problems [12].

We illustrate our procedure, through the sextic oscillator in the units $\hbar = 2m = \omega = 1$, for the purpose of comparison with the standard literature. The corresponding eigenvalue equation is given by:

$$\left[-\frac{d^2}{dx^2} + \alpha x^2 + \gamma x^6 \right] \psi(x) = E\psi(x). \qquad (30)$$

Asymptotic analysis suggests a trial wave function of the form

$$\psi(x) = e^{-bx^4} \widetilde{\psi}(x), \qquad (31)$$

which leads to,

$$\left[-\frac{d^2}{dx^2} + 2\sqrt{\gamma}\, x^3 \frac{d}{dx} + \left(\alpha + 3\sqrt{\gamma} \right) x^2 \right] \widetilde{\psi}(x) = E\widetilde{\psi}(x), \qquad (32)$$

where x^6 term has been removed by the condition $16b^2 = \gamma$. One notices that, the operator $\tilde{O} = (\alpha + 3\sqrt{\gamma})x^2 + 2\sqrt{\gamma}x^3 d/dx$ increases the degree of $\tilde{\psi}(x)$ by two, if $\tilde{\psi}(x)$ is a polynomial. Confining ourselves to polynomial solutions and assuming that the highest power of the monomial in $\tilde{\psi}(x)$ is n, one obtains

$$-\frac{\alpha}{\sqrt{\gamma}} = 2n + 3, \tag{33}$$

after imposing the condition that $\tilde{O}$ does not increase the degree of the polynomial. This is the well-known relationship between the coupling parameters of the quasi-exactly solvable sextic oscillator [12]. Taking $n = 4$ and $\gamma = 1$ for simplicity, after multiplying the above equation with x^2 :

$$\left[D(D-1) + Ex^2 + 8x^4 - 2x^5 \frac{d}{dx} \right] \widetilde{\psi}(x) = 0 \tag{34}$$

we get,

$$\widetilde{\psi_0}(x) = C_0 \left\{ \sum_{m=0}^{\infty} (-1)^m \left[\frac{1}{D(D-1)} (E_0 x^2 + 8x^4 - 2x^5 \frac{d}{dx}) \right]^m \right\} 1. \tag{35}$$

Modulo C_0, the above series can be expanded as,

$$\widetilde{\psi_0}(x) = 1 - E_0 \frac{x^2}{2!} + (E_0^2 - 16)\frac{x^4}{4!} + \left(64E_0 - E_0^3\right)\frac{x^6}{6!} + ... \tag{36}$$

The monomials having degree greater than four vanish provided, $E_0 = 0, \pm 8$. It can be explicitly checked that, for these values of E_0, Eq.(34) is satisfied. The eigenfunctions corresponding to these three values are given by,

$$\psi_{-8}(x) = e^{-x^4/4} \left[1 + 4x^2 + 2x^4 \right],$$
$$\psi_0(x) = e^{-x^4/4} \left[1 - \tfrac{2}{3}x^4 \right]$$

and

$$\psi_{+8}(x) = e^{-x^4/4} \left[1 - 4x^2 + 2x^4 \right].$$

This procedure generalizes to a wide class of QES problems [13].

Below, we demonstrate the method of finding approximate eigenvalues and eigenfunctions for non-exactly solvable problems, using the well studied anharmonic oscillator as the example [13]:

$$\left[-\frac{d^2}{dx^2} + \alpha x^2 + \beta x^4 - E_n \right] \psi_n(x) = 0. \tag{37}$$

Proceeding as before, $\psi_0(x)$ can be written as,

$$\psi_0(x) = C_0 \left\{ \sum_{m=0}^{\infty} (-1)^m \left[\frac{1}{(D-1)D} \left(E_0 x^2 - \alpha x^4 - \beta x^6 \right) \right]^m \right\} 1, \tag{38}$$

which has an expansion in the form,

$$\psi_0(x) = 1 - \frac{E_0}{2!} x^2 + \frac{1}{4!} \left(2\alpha + E_0^2 \right) x^4 - \frac{1}{6!} \left(24\beta - (14\alpha E_0 + E_0^3) \right) x^6 + \cdots \tag{39}$$

Although a number of schemes can be devised for the purpose of approximation, we consider the simplest one of starting with a trial function $\tilde{\psi}_0(x) = \exp(-\mu x^2 - \nu x^4)$ and matching it with $\psi_0(x)$. Comparison of the first three terms yields,

$$\mu = \frac{E_0}{2!},$$
$$\frac{\mu^2}{2!} - \nu = \frac{2\alpha}{4!} + \frac{E_o^2}{4!}$$

and

$$\mu\nu - \frac{\mu^3}{3!} = \frac{\beta}{30} - \frac{(14E_0 + E_0^3)}{6!}. \tag{40}$$

The resulting cubic equation in energy, $E_0^3 - E_0\alpha = 3\beta/2$, leads to one real root and two complex roots. Choosing the real root on physical grounds, one obtains,

$$E_0 = \frac{2^{1/3}\alpha}{A} + \frac{A}{3.2^{1/3}},$$

where $A = \left[40.5\beta + (1640.25\beta^2 - 108\alpha^3)^{1/2} \right]^{1/3}$. The value of E_0, obtained in the weak coupling regime, matches reasonably well with the earlier obtained results [14]. An approximate ψ_0 can be obtained from Eq.(39). One can easily improve upon the above scheme by taking better trial wave functions. Similar analysis can be carried out for the excited states. The above expansion of the wave function is well suited for a numerical treatment. For example, an accurate numerically determined energy value can lead to a good approximate wave function.

5   Many-Body Interacting Systems

In this section, we will be dealing with correlated many-body systems, particularly of the Calogero-Sutherland [15] and Sutherland type [16]. As will be seen soon, the wave functions of these interacting N-particle systems do not separate into product of single particle

wavefunctions. This brings in correlations between different particles. These models have found application in diverse branches of physics like fluid flow, random matrix theory, novel statistics, quantum Hall effect and others [3, 17].

We start with the relatively difficult Sutherland model, where the particles are confined to a circle of circumference L. The two-body problem treated explicitly below, straight-forwardly generalizes to N particles. The Schrodinger equation is given by (in the units $\hbar = m = 1$),

$$\left[-\frac{1}{2} \sum_{i=1}^{2} \frac{\partial^2}{\partial x_i^2} + \beta(\beta - 1)\frac{\pi^2}{L^2}\frac{1}{\sin^2[\pi(x_1 - x_2)/L]} - E_\lambda \right] \psi_\lambda(\{x_i\}) = 0 \qquad . \tag{41}$$

Taking, $z_j = e^{2\pi i x_j/L}$ and writing $\psi_\lambda(\{z_i\}) = \prod_{i,i \neq j} z_i^{-\beta/2}(z_i - z_j)^\beta J_\lambda(\{z_i\})$, the above equation becomes,

$$\left[\sum_{i=1}^{2} D_i^2 + \beta\frac{z_1 + z_2}{z_1 - z_2}(D_1 - D_2) + \tilde{E}_0 - \tilde{E}_\lambda \right] J_\lambda(\{z_i\}) = 0 \qquad , \tag{42}$$

where, $D_i \equiv z_i\frac{\partial}{\partial z_i}$, $\tilde{E}_\lambda \equiv 2(\frac{L}{2\pi})^2 E_\lambda$, $\tilde{E}_0 \equiv 2(\frac{L}{2\pi})^2 E_0$ and $E_0 = (\frac{\pi}{L})^2\beta^2$, is the ground state energy. Here, $J_\lambda(\{z_i\})$ is the polynomial part, which in the multivariate case is the well known Jack polynomial [8]. λ is the degree of the symmetric function and $\{\lambda\}$ refers to different partitions of λ. $\sum_i D_i^2$ is a diagonal operator in the space spanned by the monomial symmetric functions, $m_{\{\lambda\}}$, with eigenvalues $\sum_{i=1}^{2} \lambda_i^2$. A monomial symmetric function is a symmetrized combination of monomials of definite degree. For example for two particle case, there are two monomial symmetric functions having degree two. These are $m_{2,0} = x_1^2 + x_2^2$ and $m_{1,1} = x_1 x_2$. Readers are referred to Ref. [8] for more details about various symmetric functions and their properties. Rewriting Eq.(42) in the form,

$$\left[\sum_i (D_i^2 - \lambda_i^2) + \beta\frac{z_1 + z_2}{z_1 - z_2}(D_1 - D_2) + \tilde{E}_0 + \sum_i \lambda_i^2 - \tilde{E}_\lambda \right] J_\lambda(\{z_i\}) = 0 \qquad , \tag{43}$$

one can immediately show that,

$$J_\lambda(\{z_i\}) = C_\lambda\left\{ \sum_{n=0}^{\infty} (-1)^n \left[\frac{1}{\sum_i(D_i^2 - \lambda_i^2)}\left(\beta\frac{z_1 + z_2}{z_1 - z_2}(D_1 - D_2) + \tilde{E}_0 + \sum_i \lambda_i^2 - \tilde{E}_\lambda \right) \right]^n \right\}$$
$$\times m_\lambda(\{z_i\}) \quad . \tag{44}$$

For the sake of convenience, we define

$$\hat{S} \equiv \left[\frac{1}{\sum_i (D_i^2 - \lambda_i^2)}\hat{Z}\right] \quad ,$$

$$\text{and} \quad \hat{Z} \equiv \beta\frac{z_1 + z_2}{z_1 - z_2}(D_1 - D_2) + \tilde{E}_0 + \sum_i \lambda_i^2 - \tilde{E}_\lambda \quad . \tag{45}$$

The action of $\hat{S}$ on $m_\lambda(\{z_i\})$ yields singularities, unless one chooses the coefficient of m_λ in $\hat{Z}\, m_\lambda(\{z_i\})$ to be zero; this condition yields the eigenvalue equation

$$\tilde{E}_\lambda = \tilde{E}_0 + \sum_i (\lambda_i^2 + \beta[3 - 2i]\lambda_i) \quad .$$

Using the above, one can write down the two particle Jack polynomial as,

$$J_\lambda(\{z_i\}) = \sum_{n=0}^{\infty} (-\beta)^n \left[\frac{1}{\sum_i(D_i^2 - \lambda_i^2)}(\frac{z_1 + z_2}{z_1 - z_2}(D_1 - D_2) - \sum_i(3 - 2i)\lambda_i)\right]^n$$
$$\times m_\lambda(\{x_i\}) \quad . \tag{46}$$

Starting from $m_{2,0} = z_1^2 + z_2^2$, it is straightforward to check that

$$\begin{aligned}
\hat{Z}m_{2,0} &= 4\beta(z_1 + z_2)^2 = 4\beta m_{1,0}^2 \\
\hat{S}m_{2,0} &= \frac{1}{\sum_i(D_i^2 - 4)}(4\beta m_{1,0}^2) = -2\beta m_{1,0}^2 \quad , \\
\hat{S}^n m_{2,0} &= -2(\beta)^n m_{1,0}^2 \quad \text{for} \quad n \geq 1 \quad .
\end{aligned}$$

Substituting the above result in Eq.(44), apart from C_2, one obtains

$$\begin{aligned}
J_2 &= m_{2,0} + \left(\sum_{n=1}^{\infty}(-1)^n(-2)(\beta)^n\right)m_{1,0}^2 \\
&= m_{2,0} + 2\beta\left(\sum_{n=0}^{\infty}(-\beta)^n\right)m_{1,0}^2 \\
&= m_{2,0} + \frac{2\beta}{1 + \beta}m_{1,0}^2 \tag{47}
\end{aligned}$$

which is the desired result. The above approach can be generalized to the N-particle case.

Another class of many-body problems, which can be solved by the present approach is the Calogero-Sutherland model (CSM) and its generalizations [18]. Proceeding along the line, as for the Sutherland model, one finds the eigenvalues and eigenfunctions for the CSM.

The Schrodinger equation for the CSM in the previous units, is given by,

$$\left[-\frac{1}{2} \sum_{i=1}^{N} \frac{\partial}{\partial x_i^2} + \frac{1}{2} \sum_{i=1}^{N} x_i^2 + \frac{g^2}{2} \sum_{\substack{i,j \\ i \neq j}} \frac{1}{(x_i - x_j)^2} - E_n \right] \psi_n(\{x_i\}) = 0 \qquad (48)$$

where the wave function is of the form

$$\psi_n(x) = \psi_0 P_n(\{x_i\}) = ZG P_n(\{x_i\}). \qquad (49)$$

Here $Z \equiv \prod_{i<j}(x_i - x_j)^\beta$, $G \equiv \exp\left\{-\frac{1}{2}\sum_i x_i^2\right\}$, $g^2 = \beta(\beta - 1)$ and $P_n(\{x_i\})$ is a polynomial. We specifically note that the presence of Z in $\psi_n(x)$, as also the polynomial part $P_n(\{x_i\})$ prevents the wavefunction to be separable into individual particle wavefunctions. This indicates the correlated nature of this many-body wave function. After removing the ground state, the polynomial $P_n(\{x_i\})$ satisfies,

$$\left[\sum_i x_i \frac{\partial}{\partial x_i} + E_0 - E_n - \frac{1}{2} \sum_i \frac{\partial^2}{\partial x_i^2} - \beta \sum_{i \neq j} \frac{1}{(x_i - x_j)} \frac{\partial}{\partial x_i} \right] P_n(\{x_i\}) = 0, \qquad (50)$$

where $E_0 = \frac{1}{2}N + \frac{1}{2}\beta N(N-1)$. Defining

$$\tilde{A}(\beta) \equiv \frac{1}{2} \sum_i \frac{\partial^2}{\partial x_i^2} + \beta \sum_{i \neq j} \frac{1}{(x_i - x_j)} \frac{\partial}{\partial x_i} \quad (51)$$

one can easily see, following the procedure adopted for the Hermite DE that,

$$P_n(\{x_i\}) = C_n e^{-\frac{\tilde{A}(\beta)}{2}} m_{\{n\}}(\{x_i\}), \qquad (52)$$

where $m_{\{n\}}(\{x_i\})$ is a monomial symmetric function of degree n. The corresponding energy is given by

$$E_n = E_o + n. \qquad (53)$$

One can use the above procedure to solve many other interacting systems.

6 Conclusion

In conclusion, we have presented a novel scheme to treat exactly, quasi-exactly and non-exactly solvable problems, which also extends to a wide class of many-body interacting systems. The procedure can be used for the construction of the ladder operators for various orthogonal polynomials and the quantum systems associated with them.

The approximation scheme presented needs further refinement. It should be analyzed in conjunction with computational tools for finding its efficacy as compared to other methods. The many-body problems presented here have deep connection with diverse branches of physics and mathematics. The fact that the procedure employed for solving them, connects the solution space of the problem under study to the space of monomials, will make it useful for constructing ladder operators for the many-variable case. This will throw light on the structure of the Hilbert space of these correlated systems. Some of these questions are currently under study and will be reported elsewhere.

References

[1] W. Miller Jr., *Symmetry and Separation of Variables (Encyclopedia of Mathematics and its Applications Volume 4)*, Cambridge University Press, 1984 (ISBN: 978-0521302241).

[2] N. Gurappa and P. K. Panigrahi, *Phys. Rev.* **B 62**, 1943 (2000);
N. Gurappa, P. K. Panigrahi, T. Shreecharan and S.Sree Ranjani in *Frontiers of Fundamental Physics 4*, Eds: B. G. Sidharth and M. V. Altaisky, Kluwer Academic Plenum Publishers, New York, 269 (2001);
M. Ezung, N. Gurappa, A. Khare and P. K. Panigrahi, Phys. Rev.**B 71**, 125121(2005).

[3] N. Gurappa and P. K. Panigrahi, *Phys. Rev.* **B 59**, R2490 (1999) and references therein.

[4] J. Mathews and R. L. Walker, *Mathematical methods of physics (2nd Edition)*, Addison-Wesley, 1970; P. M. Morse and H. Feschbach, *Methods of Theoretical Physics*, **Vol 1**, McGraw-Hill, New-York, 1953.

[5] F. M. Fernndez, *Phys. Lett.* **A 237**, 189 (1998).

[6] N. Gurappa, P. K. Panigrahi and T. Shreecharan, *J. Comp. Appl. Math.* **160,** 103 (2003).

[7] T. Shreecharan, P. K. Panigrahi and J. Banerji, *Phys. Rev.* **A 69,** 012102 (2004).

[8] I. G. Macdonald, *Symmetric Functions and Hall Polynomials*, Clarendon Press, Oxford, 1979.

[9] I. S. Gradshteyn and I. M. Ryzhik, *Tables of Integrals, Series and Products*, Academic Press Inc., 1965.

[10] L. Schiff, *Quantum Mechanics*, McGraw-Hill, New-York, 1968;
L. D. Landau and E. Lifshitz, *Quantum Mechanics*, Pergamon, New-York, 1977.

[11] M. A. Shifman, *Int. J. Mod. Phys.* **A 4**, 2827 (1989) and references therein.

[12] A. G. Ushveridze, *Quasi-Exactly Solvable Models in Quantum Mechanics*,

Inst. of Physics Publishing, Bristol, 1994.

[13] R. Atre and P. K. Panigrahi, *Phys. Lett.* **A 317**, 46 (2003).

[14] M. H. Macfarlane, *Ann. Phys.* **271**, 159 (1999) and references therein.

[15] F. Calogero, *J. Math. Phys.* **12**, 419 (1971).
B. Sutherland, *ibid.* **12**, 246 (1971); **12**, 251 (1971).

[16] B. Sutherland, *Phys. Rev.* **A, 4**, 2019 (1971); *ibid.* **5**, 1372 (1972).

[17] B. D. Simons, P.A. Lee, and B.L. Altshuler, *Phys. Rev. Lett.* **70**, 4122 (1993); *ibid.* **72**, 64 (1994).

[18] A. M. Perelomov, *Theor. Math. Phys.* **6**, 263 (1971); M. A. Olshanetsky and A. M. Perelomov, *Phys. Rep.* **94**, 6 (1983).

[19] N. Gurappa and P. K. Panigrahi, www.arXiv.org/hep-th/9908127.

Appendix-I: Use of BCH formula: Proof of Equation (5)

We have from Eq.(4) that

$$e^A B e^{-A} = B + [A, B] + \frac{1}{2}[A, [A, B]] + ... \tag{54}$$

Taking the explicit form of the L.H.S of Eq.(5), $e^{\frac{1}{4}\frac{d^2}{dx^2}}[-\frac{1}{2}\frac{d^2}{dx^2} + D - n]e^{-\frac{1}{4}\frac{d^2}{dx^2}}$, we identify

$$A = \frac{1}{4}\frac{d^2}{dx^2} \tag{55}$$

and

$$B = -\frac{1}{2}\frac{d^2}{dx^2} + D - n. \tag{56}$$

Substituting A and B in Eq.(54) one obtains

$$\left\{ -\frac{1}{2}\frac{d^2}{dx^2} + D - n \right\} + \frac{1}{4}[\frac{d^2}{dx^2}, \left(-\frac{1}{2}\frac{d^2}{dx^2} + D - n \right)] + \ldots \tag{57}$$

The second part of the above expression can be split up into three parts: the first and third parts vanish directly. The second part, using the second property of the Euler operator gives

$+\frac{1}{2}\frac{d^2}{dx^2}$, which directly cancels with the first term of the first part of the above expression yielding,

$$e^{\frac{1}{4}\frac{d^2}{dx^2}}[-\frac{1}{2}\frac{d^2}{dx^2} + D - n]e^{-\frac{1}{4}\frac{d^2}{dx^2}} = D - n, \tag{58}$$

with all the subsequent terms of Eq.(54) vanishing. This matches exactly with Eq.(5).

Appendix-II: Proof of Equation(11)

Though simple, the proof requires a little care and we need to use $F(D)x^\lambda = 0$. Acting the relevant operator on the ansatz solution, we get

$$[F(D) + P(x, \tfrac{d}{dx})]\{\sum_{m=0}^{\infty}(-1)^m[\tfrac{1}{F(D)}P(x, \tfrac{d}{dx})]^m\}x^\lambda$$

$$= F(D)[1 + \tfrac{1}{F(D)}P(x, \tfrac{d}{dx})]\{\sum_{m=0}^{\infty}(-1)^m[\tfrac{1}{F(D)}P(x, \tfrac{d}{dx})]^m\}x^\lambda$$

$$= F(D)\{\sum_{m=0}^{\infty}(-1)^m[\tfrac{1}{F(D)}P(x, \tfrac{d}{dx})]^m\}x^\lambda +$$

$$F(D)\{\sum_{m=0}^{\infty}(-1)^m[\tfrac{1}{F(D)}P(x, \tfrac{d}{dx})]^{m+1}\}x^\lambda.$$

   We split the first part into two parts, one with $m = 0$ and the second, $1 \leq m < \infty$. Renaming the variable for the second part as $p = m - 1$ and finally renaming p as m (as these are dummy summation variables), we can rewrite the last line as,

$$F(D)x^\lambda - F(D)\{\sum_{m=0}^{\infty}(-1)^m[\tfrac{1}{F(D)}P(x, \tfrac{d}{dx})]^{m+1}\}x^\lambda +$$

$$F(D)\{\sum_{m=0}^{\infty}(-1)^m[\tfrac{1}{F(D)}P(x, \tfrac{d}{dx})]^{m+1}\}x^\lambda = 0$$

where we have used the result $F(D)x^\lambda = 0$ and the second & third terms have cancelled each other.

Appendix-III: The Calogero-Sutherland and Sutherland Models: A Brief Introduction

While studying general many-body problems, exactly solvable quantum mechanical systems are of great help, since they lead to a better understanding of the role of interactions. The Calogero-Sutherland model (CSM), deals with a system of N identical particles in one

dimension interacting pairwise through a long range potential of $\frac{1}{r^2}$ type. For the Sutherland model (SM) the N-particle system is defined on a circle [16]. These systems have been widely studied and their eigenvalues and eigenfunctions are well known. Interestingly, the CSM can be exactly mapped to a set of free oscillators [3] through a similarity transformation. For the case of SM, a mapping exists, which connects it with free particles on a circle [19].

TABLE I. Some frequently encountered Diff. Eqns and their novel solutions.
Below, the differential equations from top to bottom, respectively, are Hermite, Laguerre, Legendre, Gegenbauer, Chebyshev Type I, Chebyshev Type II, Bessel, confluent hypergeometric and hypergeometric.

Differential Equation	$\mathbf{F(D)}$, $D \equiv x(d/dx)$	Solution
$\left[x\frac{d}{dx} - n - \frac{1}{2}\frac{d^2}{dx^2} \right] H_n(x) = 0$	$(D - n)$	$H_n(x) = C_n \exp\left[-\frac{1}{4}\frac{d^2}{dx^2} \right].x^n$
$\left[x\frac{d}{dx} - n - (\alpha + 1)\frac{d}{dx} - x\frac{d^2}{dx^2} \right] L_n^\alpha = 0$	$(D - n)$	$L_n^\alpha(x) = C_n \exp\left[-x\frac{d^2}{dx^2} - (\alpha + 1)\frac{d}{dx} \right].x$
$\left[x^2\frac{d^2}{dx^2} + 2x\frac{d}{dx} - n(n + 1) - \frac{d^2}{dx^2} \right] P_n(x) = 0$	$(D + n + 1)(D - n)$	$P_n(x) = C_n \exp\left[-\frac{1}{2(D+n+1)}\frac{d^2}{dx^2} \right].x^n$
$\left[x^2\frac{d^2}{dx^2} + (2\lambda + 1)x\frac{d}{dx} - n(2\lambda + n) - \frac{d^2}{dx^2} \right] \times$ $\times C_n^\lambda(x) = 0$	$(D + n + 2\lambda)(D - n)$	$C_n^\lambda(x) = C_n \exp\left[-\frac{1}{2(D+n+2\lambda)}\frac{d^2}{dx^2} \right].x^n$
$\left[x^2\frac{d^2}{dx^2} + x\frac{d}{dx} - n^2 - \frac{d^2}{dx^2} \right] T_n(x) = 0$	$(D + n)(D - n)$	$T_n(x) = C_n \exp\left[-\frac{1}{2(D+n)}\frac{d^2}{dx^2} \right].x^n$
$\left[x^2\frac{d^2}{dx^2} + 3x\frac{d}{dx} - n(n + 2) - \frac{d^2}{dx^2} \right] U_n(x) = 0$	$(D + n + 2)(D - n)$	$U_n(x) = C_n \exp\left[-\frac{1}{2(D+n+2)}\frac{d^2}{dx^2} \right].x^n$
$\left[x^2\frac{d^2}{dx^2} + x\frac{d}{dx} - \nu^2 + x^2 \right] J_{\pm\nu}(x) = 0$	$(D + \nu)(D - \nu)$	$J_{\pm\nu}(x) = C_{\pm\nu} \exp\left[-\frac{1}{2(D\pm\nu)}x^2 \right].x^{\mp\nu}$
$\left[x\frac{d}{dx} + \alpha - x\frac{d^2}{dx^2} - \gamma\frac{d}{dx} \right] \Phi(\alpha, \gamma, x) = 0$	$(D + \alpha)$	$\Phi(\alpha, \gamma, x) = C_{-\alpha} \exp\left[-x\frac{d^2}{dx^2} - \gamma\frac{d}{dx} \right].x^-$
$\left[x(1 - x)\frac{d^2}{dx^2} + (\gamma - [\alpha + \beta + 1]x)\frac{d}{dx} - \alpha\beta \right] \times$ $\times F(\alpha, \beta, \gamma, x) = 0$	$(D + \alpha)(D + \beta)$	$F(\alpha, \beta, \gamma, x) = C_{-(\alpha,\beta)} \times$ $\times \exp\left[-\frac{1}{[D+(\alpha,\beta)]}(x\frac{d^2}{dx^2} + \gamma\frac{d}{dx}) \right].x^{-(\beta,\alpha}$

The solution to the Diff Eqns provided $F(D)x^\lambda = 0$.
$[F(D) + P(x, d/dx)] y(x) = 0$, is,
$y(x) = C_\lambda \left\{ \sum_{m=0}^\infty (-1)^m \left[\frac{1}{F(D)} P(x, d/dx) \right]^m \right\} x^\lambda$,

Exact Statistical Mechanics of Particle in a box using Canonical Ensemble

R.K. Sathish[1], K. M. Udayanandan[1,a], A. Augustine. [2]

[1] Dept. of Physics,
Nehru Arts and Science College,
Kerala-671 314, INDIA,

[2]Department of Physics,
University of Kannur,
Kerala 673 635, INDIA.
[a]udayanandan_km@rediffmail.com

Abstract

Statistical mechanics has been used for obtaining thermodynamics of systems mainly with classical energy and rarely for systems with quantum energy. For most of the situations with quantum energy, evaluation of the partition function which involves summation, is done by replacing the summation by integration. This replacement kills the basic effect of quantization like zero point energy and effects like the influence of size. Here we show that Euler-Maclaurin [EM] summation formula can be used to obtain the exact statistical mechanics of particles with discrete energy. We hope this method will help undergraduates for solving, similar problems in statistical mechanics using canonical ensemble.

 PACS Nos: 05.70 a, 05.90 +m,
Keywords: Euler- Maclaurin summation formula, Particle in a box

1 Introduction

Using Statistical Mechanics[SM] we can solve a large number of physical problems like magnetism, thermionic emission, photoelectric effect etc occurring in nature. For calculating the physical properties using SM we require energy of the system which may be classical(continuous in nature) or quantum energies(discrete in nature) depending upon their circumstances [1]. The classical energies possessed by particles under different situations may be equal to $\frac{p^2}{2m}$, pc, $\frac{p^2}{2m} + \frac{1}{2}kx^2$ etc and the particles may have corresponding quantum energies $\frac{n^2h^2}{8mL^2}, \frac{nhc}{2L}$,$(n + \frac{1}{2})\hbar\omega$ where m is the mass of the particle, p is the momentum, x is the displacement, c is the velocity of light, $\hbar$ is the Dirac constant, ω is the angular frequency of the particle, L is the length of the box and n is the quantum number. One of the difficulties possessed by SM technicians is that, they are not able to solve the SM of systems with quantum energy because of the difficulty in evaluating the sum in the canonical ensemble. A quantized problem solved in SM text books completely is the case of nonrelativistic quantum harmonic oscillator[1]. In this case there is no difficulty in evaluating the partition function retaining the summation because of the availability of the Taylor series expansion method. But the simplest quantized system like Particle in a Box [PB] was not solved since the Taylor series method cannot be applied and alternate methods using Jacobian Theta function[2] and Abel-Plana formula[3]could not give complete solution. We show in com-ing sections that Euler-Macularin[EM] summation formula[4] can be used effectively to sum the partition function.

This article concerns the calculation of the partition function in equilibrium statistical mechanics, without replacing the summations by integrations; in particular, by applying the EM summation formula. Section 2 reproduces well-known results, or presents straightforward analytic calculations, without additional insight into the physics of the examined case. Section 3 is devoted to an order of magnitude estimate of the spacing among the energy levels of a non-relativistic quantum particle in a box, as an argument for treating energy as a discrete quantity in the calculation of the partition function of this model. In section 4 thermodynamics of PB is evaluated and conspicuous difference in the internal energy between systems possessing continuous and discrete energy is depicted.

2 Statistical thermodynamics of non-relativistic PB

Particle in a box is the simplest physical model which has been solved quantum mechanically, but unsolved thermodynamically with quantum energy eigenvalue values, using statistical mechanics. Statistical mechanics has been earlier used for obtaining thermodynamics of PB[1,5], but the information we will have is that of a classical particle because of the conventional technique of replacing the summation by integration for evalu-

ating the partition function. Here , we re in-spect the statistical thermodynamics of par-ticle in a box initially using classical energy $\frac{p^2}{2m}$ and then by quantum energy $\frac{n^2h^2}{8mL^2}$ by text book methods. The partition function of any classical system with energy ε_r is given by[1]

$$Q = \sum_{r}^{\infty} e^{-\beta\epsilon_r} \tag{1}$$

The partition function of any quantum sys-tem with energy ε_n is given by

$$Q = \sum_{n}^{\infty} g_I g_n e^{-\beta\epsilon_n} \tag{2}$$

where $\beta = \frac{1}{kT}$, g_I is the internal degrees of freedom, g_n is the degeneracy, k is the Boltz-mann's constant, r and n represents the cor-responding states and T is the absolute tem-perature.

2.1 Thermodynamics with classical energy

The partition function for a classical particle in 1D box is

$$Q = \int_{0}^{\infty} \frac{dpLe^{-\beta\epsilon_p}}{h}$$

where the energy of individual particle is $\epsilon_p = \frac{p^2}{2m}$. Using the standard integral

$$\int_{0}^{\infty} x^a e^{-\mu x} dx = a!\mu^{-a-1} \tag{3}$$

$$Q = \frac{L(2\pi mkT)^{\frac{1}{2}}}{h} \tag{4}$$

This can be written as

$$Q = \frac{\sqrt{\pi}}{2}\left(\frac{kT}{\epsilon_1}\right)^{\frac{1}{2}} \tag{5}$$

where ϵ_1 is equal to $\frac{h^2}{8mL^2}$.

2.2 Thermodynamics with continuous quantum energy

The partition function for particle in a box is

$$Q = \sum_{n=1}^{\infty} g_I g_n e^{-\beta\epsilon_n} \tag{6}$$

Here the energy of a particle is $\epsilon_n = \frac{n^2h^2}{8mL^2}$. We take $g_I = 1$ and $g_n = 1$ for 1 D. Assumption of continuity in energy levels leads to the re-placement of summation by integration and then the partition function becomes

$$Q = \int_{n=1}^{\infty} e^{-\beta\epsilon_n} dn$$

Using the approximation $\int_{0}^{\infty} \approx \int_{1}^{\infty}$

$$Q = \frac{\sqrt{\pi}}{2}\left(\frac{kT}{\epsilon_1}\right)^{\frac{1}{2}} \tag{7}$$

This is the same partition function we ob-tained for classical particle. Equations (5) and (7) show that both partition functions are identical and hence no new information regarding a quantum system is exhibited. This is due to the replacement of summation by integration evaluating the partition func-tion. We can evaluate the the internal energy of PB using the relation given below .

$$U = -\frac{\partial(lnQ)}{\partial\beta} = -\frac{1}{Q}\frac{\partial Q}{\partial\beta} \tag{8}$$

We get

$$U = \frac{1}{2}kT$$

This is the well known classical energy for a free particle. Here we have no information like zero point energy which is basically a quantum property.

3 Estimation of the spacing among the energy levels of a non-relativistic quantum PB

To justify our arguments for retaining the summation we make a simple calculation of the number of energy levels for systems with varying thickness. Our calculations once again demonstrate that thin or nano sized systems are basically of quantum origin.

Consider the case of a free particle confined in a box. The quantum energy

$$\epsilon_n = \frac{n^2 h^2}{8mL^2} \qquad (9)$$

where n= 1, 2, 3. . . , h is the Planck's constant , m is the mass of the confined particle and L is the length of the box. For n and $(n+1)^{th}$ levels the difference in energy is

$$\Delta E = E_{n+1} - E_n$$

$$\Delta E = ((n+1)^2 - n^2)\frac{h^2}{8mL^2}$$

$$\Delta E = (2n+1)\frac{h^2}{8mL^2}$$

Thus when L is large ΔE is small or the energy levels are closely spaced.

For one degree of freedom the average thermal energy is

$$\epsilon_{nx} = \frac{1}{2}kT$$

For a bulk material of size 10 cm, assuming room temperature as 300 K

$$\epsilon_{nx} = 2.1 \times 10^{-21} J$$

Using Eq(9) and taking mass of electron

$$m = 9.1 \times 10^{-31} kg$$

and Planck's constant $h = 6.6 \times^{-34} Js$ we get

$$n_x \approx 10^9$$

Similar calculation for a micro material with thickness $10^{-6}m$ gives n nearly equal to 15 and for a nano material gives n nearly equal to .015. With the above n when ΔE is found we get

$$\Delta E \approx 10^{-26} J$$

for bulk material

$$\Delta E \approx 10^{-25} J$$

for micro material and

$$\Delta E \approx 10^{-18} J$$

for nano material. Thus when a substance becomes nano sized the energy levels becomes 10^8 times separated.

Besides the expression for energy also shows that the difference in energy eigenvalue values increases as 'n' increases which will never lead to continuum. Hence we are forced to retain the summation while evaluating the partition function. But no simple series expansion is available to evaluate the sum. Thus we go for EM method in the following section.

4 Statistical Thermodynamics of non relativistic PB using EM method

Euler- Maclaurin formula for evaluating a sum is given by

$$\sum_{n=i}^{f} f(n) = \frac{1}{2}f(i) + \int_{i}^{f} f(x)dx - \sum_{p=1}^{\infty} \frac{B_{2p}}{2p!} f^{2p-1}(i)$$

where B_{2p} are the Bernoulli numbers with $B_2 = \frac{1}{6}$, $B_4 = \frac{-1}{30}$ and $B_6 = \frac{1}{42}$ where i and f are the initial and final values of n. For PB this formula modifies to

$$\sum_{n=1}^{\infty} f(n) = \frac{1}{2}f(1) + \int_{1}^{\infty} f(x)dx - \sum_{p=1}^{\infty} \frac{B_{2p}}{2p!} f^{2p-1}(1)$$

We plotted $\frac{U}{\epsilon_1}$ and $\frac{kT}{\epsilon_1}$ numerically using Mathematica. The plots given below show that there is clear distinction between energies without replacing summation and with summation.

Numerically we found the summation for $p = \infty$ and it is observed that for $p = 2$ onwards the plot does not vary prominantly. Since obtaining an analytic expression for partition function for large values of p is difficult we evaluate below the partition function for $p = 2$. EM formula becomes

$$\sum_{n=1}^{\infty} f(n) = \frac{1}{2}f(1) + \int_{1}^{\infty} f(x)dx - \frac{B_2}{2!}f'(1) - \frac{B_4}{4!}f'''(1))$$

we have

$$f(x) = e^{-\frac{\epsilon_1}{kT}x^2}$$

$$f'(1) = -2\left[\frac{\epsilon_1}{kT}\right]e^{-\frac{\epsilon_1}{kT}}$$

$$f'''(1) = \left[-8\left(\frac{\epsilon_1}{kT}\right)^3 + 12\left(\frac{\epsilon_1}{kT}\right)^2\right]e^{-\frac{\epsilon_1}{kT}}$$

Substituting, the partition function becomes

$$Q = \frac{\sqrt{\pi}}{2}\left(\frac{kT}{\epsilon_1}\right)^{\frac{1}{2}} + \left[-\frac{1}{90}\left(\frac{\epsilon_1}{kT}\right)^3 + \frac{1}{60}\left(\frac{\epsilon_1}{kT}\right)^2 + \frac{1}{6}\left(\frac{\epsilon_1}{kT}\right) + \frac{1}{2}\right]e^{\frac{-\epsilon_1}{kT}}$$

Using the above Q we get

$$\frac{U}{\epsilon_1} = \frac{\frac{\sqrt{\pi}}{4}\left(\frac{kT}{\epsilon_1}\right)^{\frac{3}{2}} + \left[\frac{1}{3} + \frac{2\epsilon_1}{15kT} + \frac{1}{20}\left(\frac{\epsilon_1}{kT}\right)^2 - \frac{1}{90}\left(\frac{\epsilon_1}{kT}\right)^3\right]e^{\frac{-\epsilon_1}{kT}}}{\frac{\sqrt{\pi}}{2}\left(\frac{kT}{\epsilon_1}\right)^{\frac{1}{2}} + \left[\frac{1}{2} + \frac{\epsilon_1}{6kT} + 15\left(\frac{\epsilon_1}{kT}\right)^2 - \frac{1}{90}\left(\frac{\epsilon_1}{kT}\right)^3\right]e^{\frac{-\epsilon_1}{kT}}}$$

A plot of $\frac{kT}{\epsilon_1}$ with $\frac{U}{\epsilon_1}$ is shown in Figure(1). The plot depends on ϵ_1 where ϵ_1 is equal to $\frac{h^2}{8mL^2}$ which is a function of L. Thus thermodynamics of particle in a box is size dependent which is contradicting our earlier result that internal energy of the particle in a box is only a function of temperature.

5   Conclusions

In this paper we showed that EM summation formula can be successfully used to find the thermodynamics of a system with quantized energy. In the case of particle in a box there are differences in energies at different temperatures similar to a harmonic oscillator[1]. The two curves show that there is a clear separation which is due to the zero point energy. Besides at the beginning, which is low temperature region, there is conspicuous difference.

We are familiar with different applications of quantum harmonic oscillators in SM and hence we hope that the exact thermodynamics of PB also will play some key roles in SM of nanosized systems.

References

[1] R.K.Pathria "Statistical Mechanics" Second Edition,Butterworth/Heinmann (1999)

[2] M.I.Molina, arXive:physics/9704006v1 [physics.Ed-ph]

[3] Michal Demetri an, arXive:physics/0303110v4 [physics.Ed-ph]

[4] Arfken and Weber,"Mathematical Methods for Physicists", Academic Press, Sixth edition (2005)

[5] Fundamentals of Statistical and Thermal Physics, F. Re if, McGraw-Hill Series (2008)
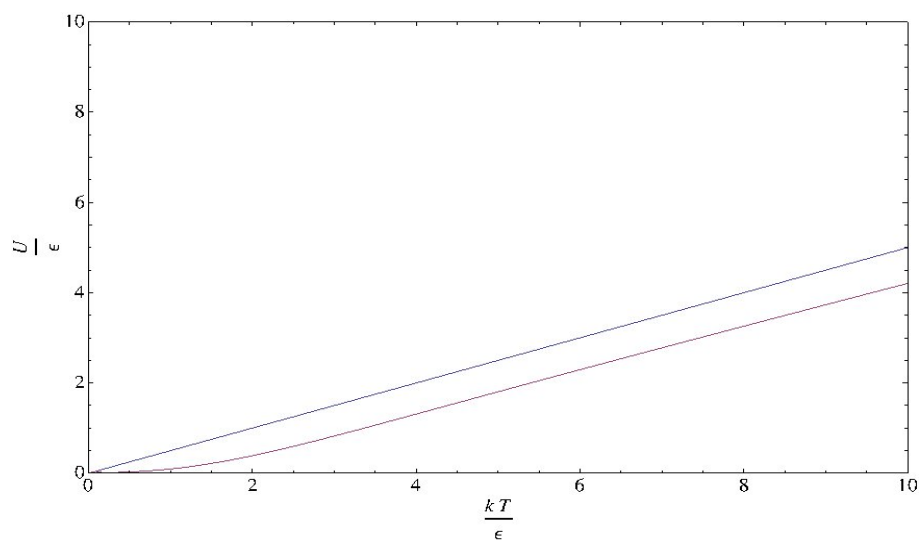
Figure 1: $\frac{kT}{\epsilon_1}$ versus $\frac{U}{\epsilon_1}$ curve for particle in a box using E M series expansion. The upper curve is for classical energy and lower curve is for quantum energy

Computer generated Fourier holograms for undergraduate optics laboratory

A. Vijayakumar[1], B. J. Jackin [2] and P. K. Palanisamy[3]

[1]Department of Electrical Engineering
Indian Institute of Technology Madras
Chennai 600036, India.

[2]Center for Optics Research and Education,
Utsunomiya University, Japan

[3]Department of Physics
Anna University
Chennai 600025, India.

(*Submitted* 23-08-2012)

Abstract

A computer simulation technique for generating Fourier holograms using the Fraunhofer diffraction formula is discussed. These generated Fourier holograms were verified for optical reconstruction after printing them on to films and the results were compared with the simulated reconstruction. A detailed analysis was done on the computation and optical reconstruction. Filtering techniques were employed and corresponding reconstructions were verified. MATLAB was used for computer simulation. The algorithm of the MATLAB program is discussed. Using this technique, computer generated holograms can be easily generated in a PC even at undergraduate level.

1. Introduction

Holography is popularly known as the art of recording and reproducing a 3D image or scene very close to its reality. But, from the scientific perspective, "it is the recording of both amplitude and phase information contained within a propagating wavefront over a certain region of space". The earliest methods of constructing optical holograms involves the use of highly coherent light sources, high resolution recording materials, optical elements and vibration isolation table.

The optical holography technique also demands the presence of the real object (for which the hologram is to be made). In optical holography recording, light from a coherent laser source scattered from the object is made to interfere with a reference light derived from the same source. The recorded fringe

pattern when illuminated by the same reference light generates the object wavefront (3D image). Nevertheless, in computer simulated holography, the entire recording and reconstruction processes are simulated using diffraction formula. The first computer generated hologram (CGH) was made by A.W.Lohmann and D.P. Paris in 1967[1]. Thereafter this technique has undergone many improvements and changes in both procedure and computational techniques [2].

Once the choice of the diffraction formula has been made, then the choice of suitable computer implementation procedures should be made. The computing environment should be chosen such that it improves speed, accuracy and also cost efficiency for that type of simulation method. In our work, the Fraunhofer diffraction formula is used for

simulation. The holograms thus generated using diffraction formula can be used for optical reconstruction.

This paper consists of four parts. The first part describes the theory of our work. The second part gives the complete details of the simulation algorithm. The third part of the paper gives the details about the optical reconstruction. The final part contains the MATLAB code which can be used for reproducing our results.

2.   Theory

According to scalar diffraction theory, the emanating wavefronts are spherical [3,4]. The scalar diffraction theory at the end of Fresnel approximation reshapes the spherical wavefronts to parabolic wavefronts [5]. Since the parabolic approximation is valid only for small diffraction angles this approximation is also called as paraxial approximation. The far field approximation of Fresnel diffraction formula yields the Fraunhofer diffraction formula. The Fraunhofer diffraction formula is the Fourier transform of the aperture distribution. This formula greatly simplifies the calculations compared to Huygen – Fresnel diffraction formula. The simulation is employed using a simple algorithm in MATLAB language. In the following theory, the notations followed in [5] are used.

Let the object be a planar transparent object in an opaque (ξ,η) plane called as the object plane. Let (x,y) be the hologram plane which is at a distance z from the object plane. The amplitude transmittance functions for the object and the reference waves are $T_o(\xi,\eta)$ and $T_r(\xi,\eta)$ respectively. The Fresnel diffraction formula is given by

$$U(x,y) = \frac{e^{jkz}e^{j\frac{k}{2z}(x^2+y^2)}}{j\lambda z} \int\limits_{-\infty}^{+\infty}\int\limits_{-\infty}^{+\infty} \left\{ T(\xi,\eta)\exp\left[j\frac{k}{2z}(\xi^2+\eta^2)\right]\right\}$$
$$\exp\left[-j\frac{2\pi}{\lambda z}(x\xi+y\eta)\right]d\xi d\eta \quad (1)$$

$T(\xi,\eta)$ in equation (1) must be replaced by $T_o(\xi,\eta)$ and $T_r(\xi,\eta)$ for calculation of the diffracted field amplitude profile for object and reference respectively. The equivalent experimental set up

(for recording hologram) for the computer simulation discussed in this paper is the inline hologram recording set up as shown in figure 1.
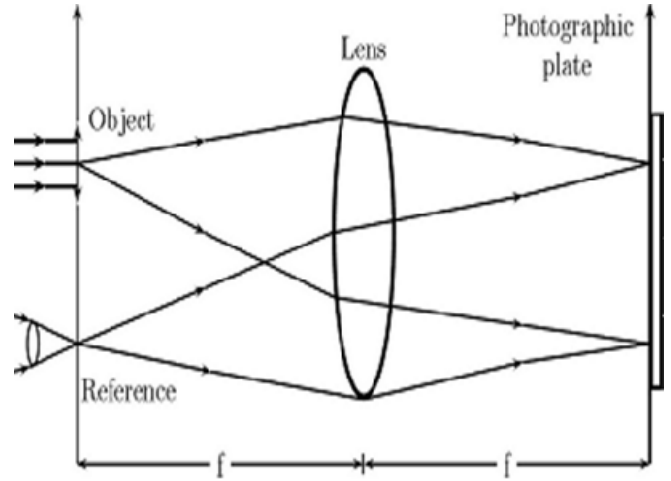

FIG.1 Hologram recording setup

The Fraunhofer diffraction formula relates the far field amplitude $U(x,y)$ (at the hologram plane) to the object plane aperture by the equation (2).

$$U(x,y) = \frac{e^{jkz}e^{j\frac{k}{2z}(x^2+y^2)}}{j\lambda z} \int\limits_{-\infty}^{+\infty}\int\limits_{-\infty}^{+\infty} T(\xi,\eta)$$
$$\exp\left[-j\frac{2\pi}{\lambda z}(x\xi+y\eta)\right]d\xi d\eta \quad (2)$$

The above equation is evaluated at spatial frequencies $f_x = x/\lambda z$ [=cos (θ_x/λ)], $f_y = y/\lambda z$ [=cos (θ_y/λ)]. Neglecting the phase factors outside the integral, the kernel that transforms $T(\xi,\eta)$ to $U(x,y)$ is the kernel of 2D Fourier transform. Fraunhofer diffraction formula is obtained from Fresnel Integral of diffraction by the following condition

$$\frac{k}{2z}\left[\xi^2 + \eta^2\right]_{max} << 1 \quad (3)$$

i.e., for λ=632.8 nm and aperture radius of 0.01 m, z >> 1500 m. In the laboratory, the above condition is achieved by introducing a convex lens between the object plane and hologram plane such that the hologram plane coincides with the back focal plane of the lens.

The quadratic phase factor produced by the lens cancels out the phase $j(k/2z)\left[\xi^2+\eta^2\right]$. As a result,

the parabolic wavefronts reduce to plane wavefronts. The Fraunhofer diffraction equation reduces to the equation (2).

In holography, the interference pattern between the object and reference wave is recorded which is called as the hologram. In computation, the interference is obtained by the addition of the wave fields of the object and reference at the image plane. The wave fields of the object and reference at the image plane can be calculated by the formula given in [3].

By using the Linearity theorem of Fourier Transform, the two transfer functions can be added first and the sum of their wave fields at the image plane can be calculated. However, in the MATLAB code given, the fields are calculated separately and added finally. This helps to verify the program's outcome at each level.

$$U(x,y)=\frac{e^{jkf}e^{j\frac{k}{2f}(x^2+y^2)}}{j\lambda f}\int\limits_{-\infty}^{+\infty}\int\limits_{-\infty}^{+\infty}\left[T_o(\xi,\eta)+T_r(\xi,\eta)\right]$$
$$\exp\left[-j\frac{2\pi}{\lambda f}(x\xi+y\eta)\right]d\xi d\eta \tag{4}$$

In the real world, the measurable quantity is the intensity of light. So, when the intensity of the above expression is considered, the exponential terms outside the integral vanish.

To simplify the problem, the reference beam is considered as a plane wave in the image plane. As explained earlier, the set up for recording and reconstruction includes a convex lens such that the image plane is at the focus of the lens. Hence, a point source is chosen as the reference, which, upon Fourier transform, yields uniform illumination in the image plane. Mathematically, Dirac delta function, when Fourier transformed, produces a constant i.e., independent of the position in the image plane in spatial domain.

The intensity distribution is calculated in the image plane from equation (5).

$$I=UU^* \tag{5}$$

The above equation gives the intensity distribution in the hologram. Hence, the transmission function $T(x,y)$ is proportional to the intensity distribution. Details of the derivation are given in [6].

The reconstruction is done by evaluating the function $T(x,y)$ using the Fraunhofer diffraction formula. This is given in equation (6)

$$U(u,v)=\frac{e^{jkf}e^{j\frac{k}{2f}(u^2+v^2)}}{j\lambda f}\int\limits_{-\infty}^{+\infty}\int\limits_{-\infty}^{+\infty}T(x,y)$$
$$\exp\left[-j\frac{2\pi}{\lambda f}(xu+yv)\right]dxdy \tag{6}$$

Again as explained earlier, the exponential term before the integral vanishes when the intensity is calculated. The result of the integration yields four terms. The first term corresponds to the Fourier transform of a constant. The second term is the autocorrelation function of $T_o(\xi,\eta)$ which produces a peak at the geometric center of the observation plane which will be removed by filtering. The third and fourth terms are of interest in holography and correspond to the interference between the object wave and reference wave from the point source. The third and fourth terms are

$$K1^*\int\limits_{-\infty}^{+\infty}\int\limits_{-\infty}^{+\infty}\left[\int\limits_{-\infty}^{+\infty}\int\limits_{-\infty}^{+\infty}[T_o(\xi,\eta)]\exp\left[-j\frac{2\pi}{\lambda f}(x\xi+y\eta)\right]d\xi d\eta\right]$$
$$\exp\left[j\frac{2\pi}{\lambda f}(x\xi+y\eta)\right]\times\exp\left[-j\frac{2\pi}{\lambda f}(xu+yv)\right]dxdy$$
$$\text{and} \tag{7}$$

$$K1\int\limits_{-\infty}^{+\infty}\int\limits_{-\infty}^{+\infty}\left[\int\limits_{-\infty}^{+\infty}\int\limits_{-\infty}^{+\infty}[T_o(\xi,\eta)]\exp\left[-j\frac{2\pi}{\lambda f}(x\xi+y\eta)\right]d\xi d\eta\right]^*$$
$$\exp\left[-j\frac{2\pi}{\lambda f}(x\xi+y\eta)\right]\times\exp\left[-j\frac{2\pi}{\lambda f}(xu+yv)\right]dxdy$$

The evaluation of the two integrals yields two separate real images of the object at the (u,v) plane. In other words, two transmittance functions of the object are reproduced at the back focal plane of the lens such that one is the conjugate of the other. A detailed discussion is given in [6].

3. The simulation algorithm

The simulation Algorithm has two parts. The first part explains the simulation algorithm that is applicable to all computer programming languages. The second part gives the details of MATLAB code to perform the above simulation. Detailed information of sampling is given in [7].

Part – 1

The object and reference sizes must be chosen in accordance with the computation speed of the PC. Every computer language has its own merits and demerits. One of the well-known restrictions present in most of the languages is that when FFT of matrices are calculated, the matrix size is needed to be of the form 2^n. Let N x N be the size of the matrix.

The step by step procedure is given below

STEP – 1 Construction of Transfer function of Reference and Object

The reference as stated earlier, is the Dirac delta function. The transfer function of the matrix can be generated by making only one element of the square matrix as constant and the rest of the elements zero. There is no restriction in choosing the position. Nonetheless, if the center i.e $(((N/2)+1),((N/2)+1))$ is selected, it simplifies future hologram reconstruction. The object can be either generated or loaded. For simpler objects like an alphabet it is easier to generate and this method directly gives the matrix. In the case of other objects, like pictures, loading the image is necessary. The loaded image is then converted into a matrix for further manipulation. The resulting two matrices correspond to the transfer functions $T_o(\xi,\eta)$ and $T_r(\xi,\eta)$ in the object plane.

STEP – 2 Calculation of the Far field Amplitude $U(x,y)$

The far field amplitude calculation based on the Fraunhoffer diffraction formula is the Fourier Transform operation. Numerically, Fourier Transform integral is solved using the Discrete Fourier Transform algorithm (DFT). But, DFT calculation increases time considerably proportional to N^2. The speed of computation is increased by the Cooley – Turkey Algorithm called as the Fast Fourier Transform algorithm. This FFT computation time is proportional to $N \log N$. This is used to calculate the far field amplitude $U(x,y)$.

If $G(x,y)$ is the Fourier transform of $F(\xi,\eta)$, then

$$G(x+pN, y+qN) = \frac{1}{N}\sum_{\xi=0}^{N-1}\sum_{\eta=0}^{N-1}F(\xi,\eta)$$

$$\exp\left\{\frac{-2\pi i}{N}(x\xi+y\eta)\right\}\times\exp\left\{-2\pi i(p\xi+q\eta)\right\} (8)$$

for $x,y = 0,1,...N-1$

for all integer values of x, y, ξ, η, p and q, the second exponential term is 1. Thus

$$G(x+pN, y+qN) = G(x,y) \qquad (9)$$

In the case of continuous signals, the origin of the transform domain is at its geometrical center. In Fraunhofer diffraction also, the zero frequency term is at the center of the display. In DFT, the origin can be shifted to the center, by reordering the transform coefficients. The reordering is performed by multiplying the matrix by $(-1)^{\xi+\eta}$. For $p=q=0.5$,

$$G(x+\frac{N}{2}, y+\frac{N}{2}) = G(x+pN, y+qN)\times(-1)^{\xi+\eta} \ (10)$$

The Fourier Transforms of the object and reference waves have complex values and cannot be imaged. So, the square of the absolute values of the amplitudes (Intensity) is imaged.

Fourier transform, when discretized with periodic sampling, is only the Fourier series representation of the 2D object. In our case, the matrix representing the object is real. The matrix contains N^2 elements. When Fourier transformed, the

matrix becomes complex with $2N^2$ elements. It seems as if the dimension has increased but, in reality, it has not, as the Fourier transform exhibits the property of conjugate symmetry.

$$G^*(x,y) = G(-x, -y) \qquad (11)$$

Due to this, almost 50% of the samples are not needed and can be generated from other samples. This is the property responsible for twin images during reconstruction.

STEP – 3 Hologram construction and spatial filtering

The Hologram is the addition of far fields of the object and reference waves i.e interference. The Fourier transforms of the reference and object matrices are added. The square of the absolute values of the resulting matrix is imaged. The autocorrelation term derived above peaks at the center of the pattern during reconstruction. To reduce the intensity of the peak at the center, spatial filtering is done. The intensity of the Fourier transformed object matrix is subtracted from the hologram.

STEP – 4 Reconstruction of the hologram

The matrix corresponding to the filtered hologram is Fourier transformed. The intensity of the resulting matrix is calculated by squaring it. The matrix is imaged. The reconstructed image shows two images of the object out of which one is inverted according to the theory.

Part – 2

In many computer languages, the manipulation of FFT demands the matrix size to be 2^n. In Matlab this restriction is ruled out. However, in order to make this program compatible with other systems, matrix size of 256 x 256 (2^8) is chosen. The complete Matlab code for the simulation is given in the appendix of the paper.

STEP – 1

A matrix is generated with 256 x 256 elements. Dirac delta function is generated in Matlab by making only one element out of the total 256 x 256 elements as constant and rest of the elements are made zero. We chose the letters PKP (Pascal – Kirchoff - Poisson) as sample for analysis. The maximum value of the intensity is chosen as 100 and the minimum value is chosen as zero. In the case of loading, the opaque object plane is generated using GIMP. GIMP (version 2.6) is free software compatible with Windows. The object is made transparent in the opaque background. The image is saved as a bitmap file and it is loaded into Matlab program using the 'imread' command. The object (PKP) shown in the figure 2. is used for all analysis converting into a matrix.

FIG.2 Object

In Matlab even if the size of the object is not exactly 256 x 256 it can be used for manipulation using image resize tools (interpolation techniques). The command '*imresize*' changes the size of the object to the desired size but this process creates unwanted noisy edges. Hence, in our entire work, images are created to the

necessary sizes using GIMP and not resized using Matlab.

STEP – 2

In Matlab, '*fft*' command is used to calculate Fourier Transform. In our case we need to use '*fft2*' which is the command used to calculate 2D Fourier transform. In order to make the diffraction patterns to be centered '*fftshift*' command is used after all '*fft2*' operations. The command '*fftshift*' is equivalent to multiplying the matrix by $(-1)^{\xi+\eta}$.

STEP – 3

The addition of the far field matrices of the object and reference is performed by matrix addition. The resulting matrix is the hologram matrix. The square of the matrix (every element multiplied on to itself and not usual matrix multiplication) gives the intensity values across the hologram plane. This kind of multiplication is done by using the (.*) command and not the (*) command. Filtering is done, using matrix subtraction. The matrix is imaged using '*imagesc*' command instead of the usual '*image*' command. This operation scales the pixel values of the matrix and displays the image. The hologram without and with filtering and their respective reconstructions are shown in the figure 3. The corresponding optical reconstruction is shown in figure 4.

FIG.3 (a) Hologram without filtering (b) Reconstruction of hologram without filtering (c) Hologram with filtering (d) Reconstruction of hologram with filtering
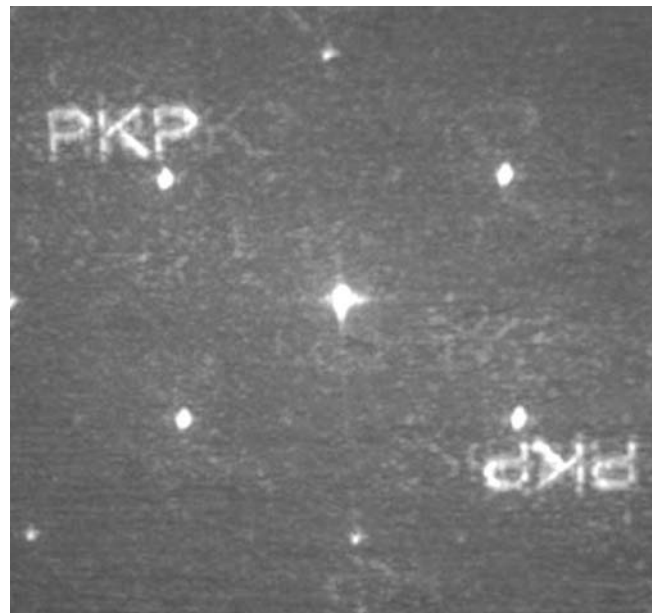

FIG.4 Result of optical reconstruction

STEP – 4

In this step, again '*fft2*' command is used. This gives the complex amplitude distribution in the reconstruction plane. The matrix is squared again as explained earlier and the resulting matrix is imaged again using '*imagesc*' command. Twin images are produced. This is in complete agreement with the theory.

To display the image, '*colormap (gray)*' is used. When the intensity ratio is varied, the reconstructed image contrast varies. In some cases, it is necessary to use '*mat2gray*' for saving the reconstructed image. For some intensity ratios, the image is fully opaque in Matlab display but is visible when equalized in GIMP. Nevertheless, for the first time Matlab user, '*colormap (prism)*' is suggested as it scales the image intensity values based on color and would not mislead the user. Instead of '*image*' command '*imagesc*' command is used to increase the visibility. The command '*subplot*' is used for viewing all results in the same page by partitioning it. Figure-5 shows the
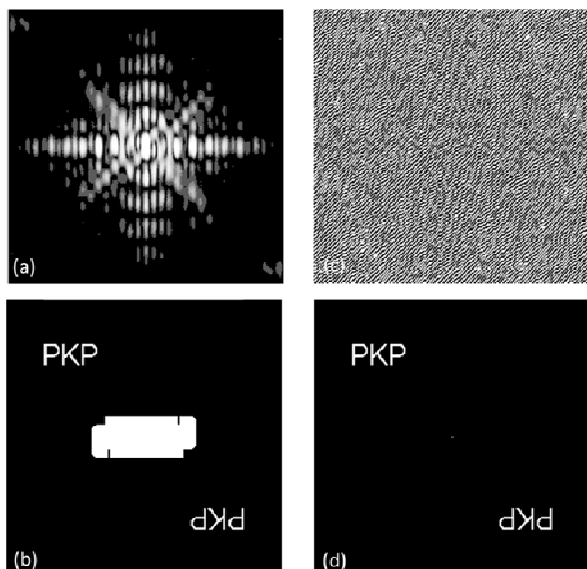
reconstructed image with high and low pass filtering. The distribution of the frequency components in Fourier domain can be obtained from any standard Digital Signal Processing (DSP) book. The high pass filtering is achieved by using only the borders of the hologram for reconstruction and vice versa for low pass filtering. The matlab simulation of the high pass and low pass filtering is shown in figure 5.
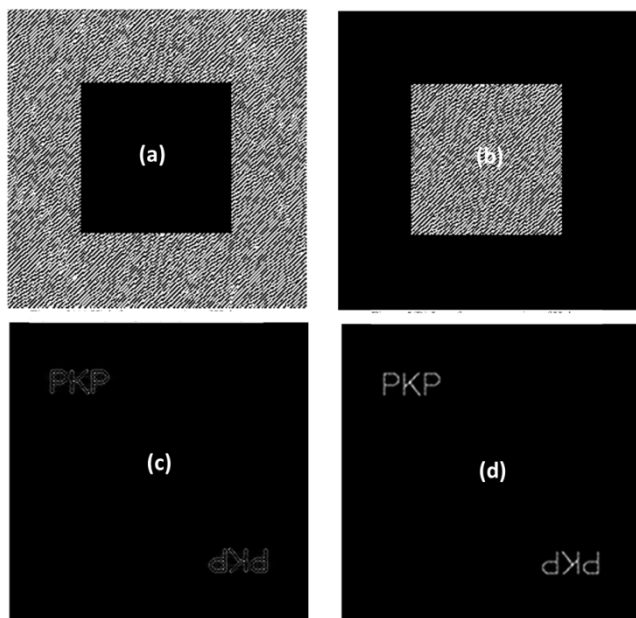
FIG.4 (a) Hologram with low frequency components removed (b) Hologram with higher frequency components (c) Reconstructed image for high pass filtering (d) Low pass filtering

When a photograph is torn into pieces, from one of the pieces, retrieval of full information is not possible. But, in a hologram, when broken into pieces, every single piece has the full information. This quality of the hologram reconstruction variation is demonstrated in computer generated Fourier holograms by reconstructing 64 x 64, 128 x 128, 192 x 192, sizes of the original 256 x 256 hologram. The convergence of the reconstructed image towards the original image with the increase in size of the hologram is visible from figure 5. The optical reconstruction is also in complete agreement with the simulation. The reconstruction images vary depending upon the position of the area in the hologram used which is evident from the filtering discussed above. In our

case, the hologram areas from the corner are used for reconstruction.

The entire simulation is done using Matlab language - Version 6. The computer we used has a RAM of 512 MB and operating system is Windows XP. Hence, the computation speed is quite high.
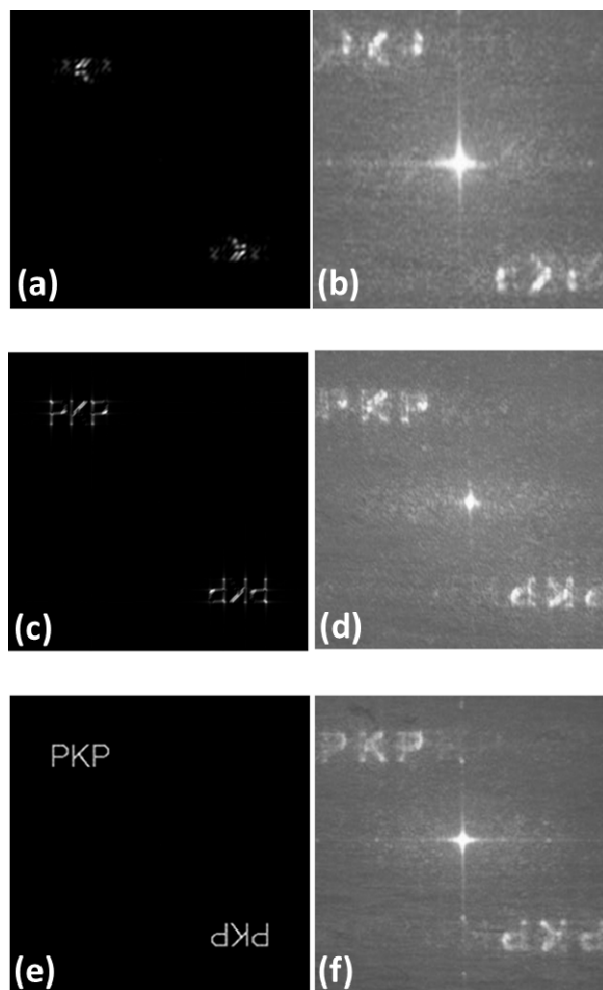

FIG.5 (a) (c) and (e) Computer reconstruction for 64 x 64, 128 x 128 and 192 x 192 hologram sizes (b) (d) and (f) Optical reconstruction for 64 x 64, 128 x 128 and 192 x 192 hologram sizes

4. Optical reconstruction

The image thus generated is transferred to the film with a resolution of 250 dpi and printed using offset style. This printing is very cheap and costs less than a rupee for making two holograms. This

can be done even with a Epson printer (whose minimum resolution is 360 dpi). The holograms were reduced to sizes 8 x 8 mm, 10 x 10 mm, 12 x 12 mm respectively and printed. In our case, 10 x 10 mm produced good quality reconstruction. A He-Ne laser of λ = 632.8 nm and power 17 mW is used. The schematic of optical reconstruction set up is shown in figure 6. During reconstruction, the position of the lens is varied to fit the beam size to the hologram size. This position is crucial as it decides the size of the reconstructed image. In our case, if the hologram size is greater than 10 mm, a second lens is introduced between the first lens and the screen to expand the beam and at the same time rescale the reconstructed image to viewable size.

The photograph shows multiple images reconstructed. The central image is more intense than the other images. As explained earlier, the Fourier integral, when discretized, represents the Fourier series as it is evaluated at periodic intervals. When the Fourier transform is performed again, there is multiple image formation at regular intervals of N. The spacing between the images during optical reconstruction is a constant. The reason for the multiple image formation is explained by Macgregor [8].

In another method, the image is optically reduced using lens after printing the hologram - image on a pick sheet which improves the reconstruction quality. But, this method is expensive and costs Rs.150 per hologram. In an undergraduate physics laboratory the low cost offset printed hologram is sufficient for study.
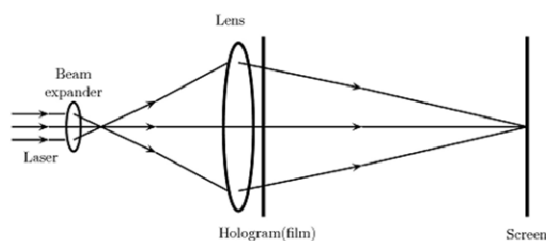

FIG.6 Schematic of optical reconstruction set up

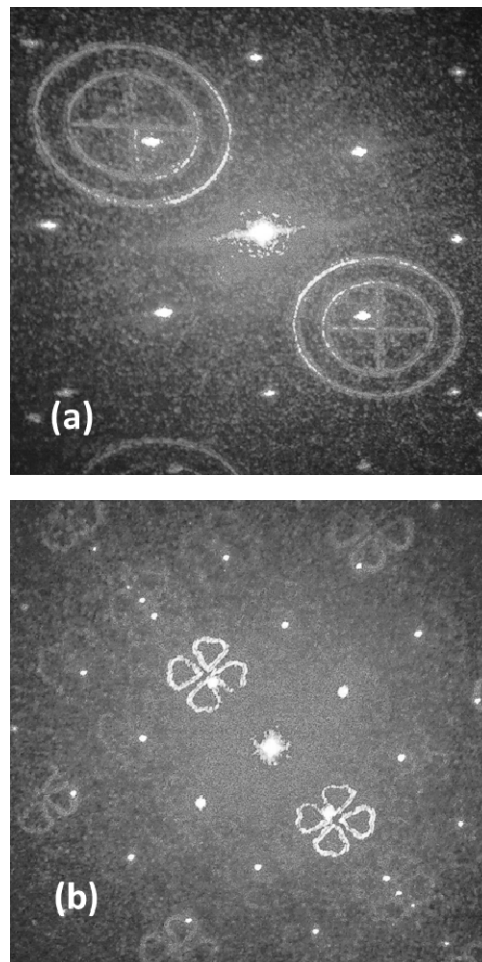A few other images after optical reconstruction is shown in figure 7.

FIG. 7 Optical reconstruction of holograms made from other images

5. Conclusion

This paper suggests simple method for the computation of Fraunhofer Holograms. The simulated reconstruction and optical reconstructions were performed to verify the results. The significances of this work may be summarized as below.

The work presented in this paper can be reproduced free of cost by anyone who has access to a computer. Since this work is focused on the undergraduate level experimentation, it is carried out without any expensive charge coupled device (CCD) chip or spatial light modulator (SLM). For

optical reconstruction alone you need a laser and beam expander. So this work also does not require a well-equipped applied optics laboratory. Hence this paper will be of interest to students, researchers and teachers who are interested in modern physics. Diffraction experiments, undergraduate and postgraduate level projects can be done using this method, free of cost and at minimum laboratory facility. So the work in this paper will also motivate academic level activities in modern optics.

We have discussed the fundamentals of computer generated holograms and demonstrated the generation and reconstruction of computer generated Fourier Holograms. We have done extensive research on computer generated holograms [9-10]. We are trying to implement the Fourier holograms generation using computer for our optics laboratory course. We believe that this paper will initiate active research in computer generated holograms in academic institutions.

The present work can also be used as a Ph.D tutorial for students interested to carry out research work in computer generated holograms. Multifunctional/ composite Fourier holograms can be designed by adding a lensing action, grating function etc to the standard hologram. The generation of composite holograms can be understood from the references [11].

Acknowledgements

The authors would like to thank 'Prof/Dr. Reviewer' for his suggestions, which improved the manuscript.

Appendix

%Fraunhoffer Hologram

%Defining the size of the object

```
clc;

clear all;
```

```
N=256;
```

%Loading the image

```
A=imread('D:\Holograms\pkp.bmp','bmp');
```
% should be suitably modified by the user

```
A=A(1:N,1:N);

A=double(A);
```

%Dirac delta function

```
B=zeros(N,N);

B(129,129)=100;
```

%To generate the diffraction pattern for the object and reference

```
A1=fftshift(fft2(A));

I1=abs(A1).*abs(A1);

B1=fftshift(fft2(B));

I2=abs(B1).*abs(B1);
```

%Hologram construction and Filtering

```
D1=A1+B1;

I3=abs(D1).*abs(D1);

I4=(I3-I1);

imwrite(I4,'D:\Holograms\pkp.bmp');
```

%Hologram reconstruction

```
D2=fftshift(fft2(I4));

I5=abs(D2).*abs(D2);

imwrite(I5, 'D:\Holograms\pkp.bmp');
```

%To see the object, reference, hologram and reconstruction

```
colormap(prism);
```

```
subplot(3,3,1);

image(A);

subplot(3,3,2);

image(B);

subplot(3,3,3);

imagesc(I1);

subplot(3,3,4);

imagesc(I2);

subplot(3,3,5);

imagesc(I4);

subplot(3,3,6);

imagesc(I5);

returnsubplot(3,3,4);

imagesc(I2);
```

References

[1]   A.W. Lohmann and D.P. Paris**,** Applied Optics, 6:1739–1748, (1967).

[2]   G. Tricoles, App. Opt, 26, 4351-4360 ,(1987).

[3]   Wolf,E.,   and   E.W.Marchand, J.Opt.Soc.Am., 54:587, (1964).

[4]   Sommerfeld A, Optics, "Lectures on Theoretical Physics", vol IV, Academic Press Inc., NewYork, (1954).

[5]   J.W. Goodman, "Introduction to Fourier Optics", San Francisco: McGraw Hill, (1968).

[6]   R.J. Collier, C.B.Burckhardt, and L.H.Lin, 'Optical Holography' (Academic, New York, 1971) (p-206-217).

[7]   F.Gascon, F.Salazar, Optik. 117 ,49–57 (2006).

[8]   A.E.Macgregor, Am.J.Phys.60, 839-846 (1992).

[9]   B.J. Jackin and T. Yatagai, Opt. Express, 18, 25546-25555, (2010).

[10]   B.J.Jackin and T. Yatagai, Appl. Opt. 50, H147 – H152, (2011).

 [11]   D. P. Godwin, D. R. Selviah,and C.D. Carey and J. E. Midwinter, 1993, (IEEE: London, UK)147-152.

Physics Through Teaching Lab XXII

MAGNET-SOLENOID INTERACTION

S. R. PATHARE, R. D. LAHANE, S. S. SAWANT[*], J. P. SHETYE

Homi Bhabha Centre for Science Education (TIFR)
V. N. Purav Marg, Mankhurd. Mumbai 400 088.
shirish@hbcse.tifr.res.in
[*]Bhavan's College, Munshi Nagar, Andheri (W), Mumbai – 400 058.
(*Submitted* Oct. - 2012)

Abstract

This is an edited version of the experiment set for the experimental examination conducted at the orientation cum selection camp held at Homi Bhabha Centre for Science Education (TIFR), Mumbai in May 2011. Students are aware that like poles of two magnets repel. In this experiment we investigate the repulsive force with respect to the distance between the two magnets. It also investigates the nature of the repulsive force between a solenoid and a magnet.

1. Introduction

It is known that like poles of two magnets repel, and unlike poles attract. The force between two current loops depends on the strengths of the currents in them, their shape, and their mutual distance. In this experiment, students are initially expected to investigate the forces between two cylindrical neodymium magnets and also forces between a magnet and a solenoid.

2. Apparatus

Two neodymium magnets, one solenoid with 3000 turns, one soft iron rod, one Hall effect sensor (UGN3501) mounted on a wooden-PVC track, one acrylic tube (with a scale pasted on it) with nylon rod and a fixing arrangement using a screw, one digital weighing balance, a pair of vernier callipers, a 9V battery, one digital multimeter, one dc power supply (15V, 1A), one retort stand with clamp, connecting wires.

3. Description of apparatus

1) Neodymium magnets:
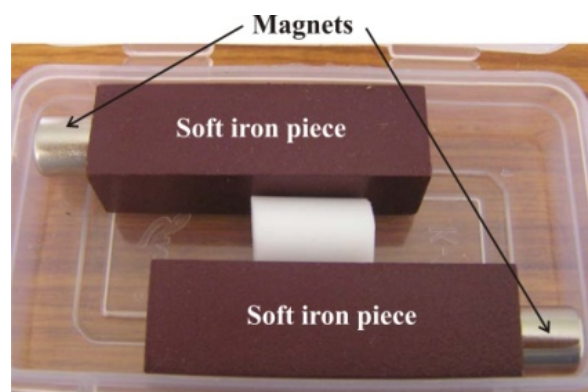
Fig.1 Neodymium magnets attached to soft iron pieces

Two neodymium magnets are provided in a box with a soft iron piece. You need to slide the magnets over the soft iron piece in order to take it out of the box. Don't drop the magnets as these are extremely brittle.

2) Solenoid:

The solenoid given to you has 3000 turns. When there is no ferromagnetic material in the core of the solenoid, it is called a solenoid with air core. Two ends of the solenoid are to be connected to the dc power supply. When not in use, the dc supply should be switched off, to avoid the heating of the solenoid.

3) Soft iron rod:

In part D of this experiment you need to replace air core with iron core. A soft iron rod is provided which can be inserted in the cavity along the axis of the solenoid. (If you face any difficulty in doing that, inform the supervisors.)
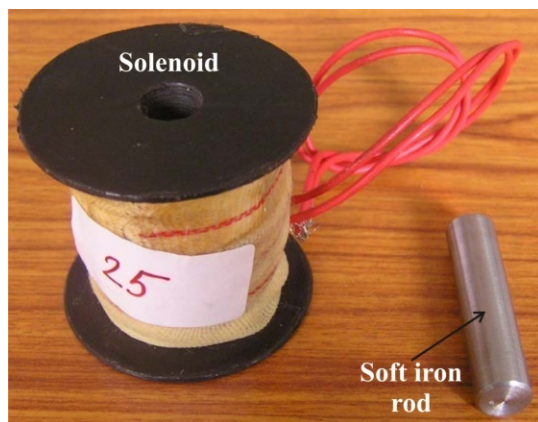
Fig.2 Solenoid and the soft iron rod

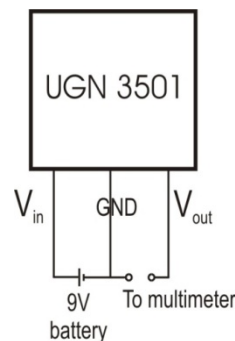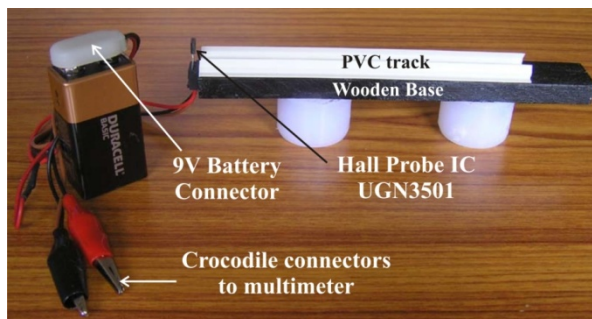4) Wooden-PVC track, acrylic tube, Hall probe assembly:

**Fig.3 Wooden-PVC track and pin connection diagram of Hall sensor**

A wooden-PVC track is provided to you for mounting an acrylic tube horizontally. Magnetic field can be measured using a Hall probe. The probe is a semiconductor device. When placed in magnetic field a small voltage is generated which is proportional to the component of magnetic field perpendicular to its plane. This voltage is amplified and read on a voltmeter. The Hall effect probe is mounted at one end of the track. The Hall effect sensor has three leads. The middle lead is common or ground terminal. Its first and common lead is connected to the 9V battery. A battery connector is provided to make the necessary connections. The third lead and common lead are connected to a multimeter used as a voltmeter with 20V dc range. The crocodile connectors are to be used to make this connection. Red and black colours of the crocodile connectors should be connected to positive and negative terminals of the voltmeter respectively.

Initially in the absence of the magnetic field, the multimeter displays voltage V_0 (nearly equal to 4.10V) volts. This may vary from probe to probe. Hence note V_0 for your instrument. In the presence of a magnetic field B, the multimeter reading changes to V. The strength of the field is obtained using the relation
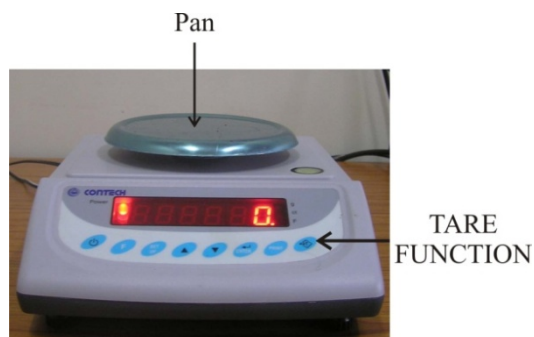
$$B = 0.14 \times \Delta V \ \text{T}$$

where $\Delta V = V - V_0$ volts. ΔV can be either positive or negative depending on the direction of B.
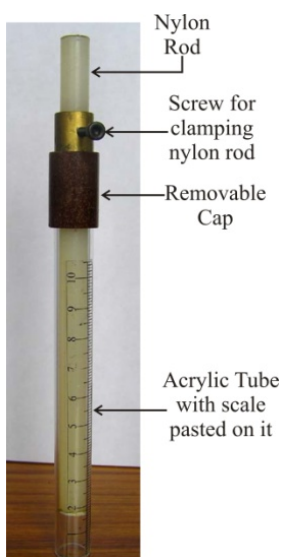
4) Acrylic Tube   5) Digital weighing balance:
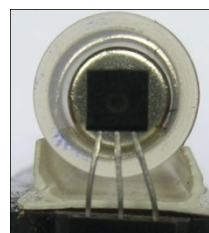

Fig.4 Acrylic tube

Fig.5 Digital weighing balance

The acrylic tube with scale printed on it is provided to make the distance measurements in various parts of this experiment. In part A, only tube is to be used (by removing the cap).

The height of the Hall effect sensor can be adjusted so that the sensor remains at the centre of the acrylic tube as shown in the Figure 6. The Figure 6a shows the acrylic tube without magnet and the Figure 6b shows the acrylic tube with magnet.
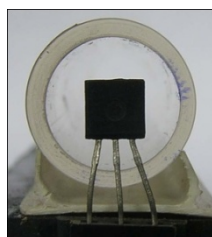
Fig.(a) without magnet

Fig.(b) with magnet

Fig.6 Hall Effect sensor adjusted at the center of the acrylic tube

This can be done by raising or lowering the sensor in the socket and simultaneously observing the reading in the multimeter. When Hall effect sensor is at the center of the tube as shown in Figure 6(b), the voltage obtained in the multimeter is maximum. Be careful while doing this as the leads of the Hall effect sensor are very thin and hence they may break if excessive and improper pressure is applied.

In this experiment the force between magnets is to be measured using digital weighing balance. The 'TARE' button is to be used for setting the reading to zero. Assume worst case error of weighing balance as $\pm$ 0.1 g.

7) DC power supply:

Figure 7: DC power supply

The dc power supply has positive (red) and negative (black) terminals. Before switching "ON" the dc supply note the following things:

a) V-coarse as well as V-fine knobs are on their "zero" positions. If they are not, then turn them anticlockwise to bring them to zero.

b) The current knob of the supply should be turned fully in clockwise direction to ensure that the current limit of the supply is high.

4. Theory

The axial magnetic field due to a cylindrical magnet of magnetic moment M at distance d along the axis from the center of the magnet can be written as

$$B = \frac{2\mu_0}{4\pi}\frac{M}{d^n} \qquad (1)$$

where the index n is expected to be an integer.

The interaction between two cylindrical magnets along their common axis can be approximately treated as dipole-dipole interaction. The force of interaction depends on the magnetic moment of the two magnets (M_1, M_2) and the separation between their centers (x).

$$F = K\frac{M_1 M_2}{x^p} \qquad (2)$$

where p is expected to be an integer.

When two magnets are placed one above the other with like poles facing each other, the upper magnet can remain suspended above the lower one at some height. Such magnetic levitation can be observed when the magnet in

the acrylic tube is placed vertically above another magnet below the tube (Figure 9). The levitation height will depend on the mass of the levitating magnet and magnetic moments of the magnets used.

A solenoid behaves like a bar magnet of magnetic moment NIA, where N is the number of turns, I is the current and A is the area of cross section of the solenoid. The force between the solenoid and the bar magnet can be written as

$$F = K\frac{(NIA)M}{x^q} \qquad (3)$$

where q is expected to be an integer.

When one of the magnets is placed in the acrylic tube in repulsive mode over the current carrying solenoid, it levitates; the weight of the magnet (mg) balances the repulsive force between the magnets.

$$mg = K\frac{(NIA)M}{x^q} \qquad (4)$$

If a soft iron rod is introduced in the core of the solenoid, the magnetic levitation increases due enhancement in the magnetic field. The above equation gets modified as

$$mg = \mu_r K\frac{(NIA)M}{x^q} \qquad (5)$$

where μ_r is the relative permeability of the soft iron rod at the given value of current.

5. Experiment

Part A: Determination of magnetic moment of the neodymium magnets

Arrange the apparatus as shown in Figure 8. Do not press the acrylic tube in the PVC track (the track may break if you do so). Connect the 9V battery to the battery connector. Connect the crocodile connectors to the digital multimeter

adjusted on an appropriate range. Carry out the centering of the Hall sensor as shown in Figure 6. Mark 1 and 2 on the magnets using the marker pen given to you. Henceforth, you can identify these magnets from their numbers.

Study the variation of the axial magnetic field as a function of distance from the center of the cylindrical magnet. While taking the observations, care must be taken such that the voltage difference, ΔV should not be less than 0.06 V.

Fig.8 Apparatus arrangement for part A

Plot a suitable graph to determine n in equation (1). Justify rounding the value of n using the uncertainty analysis.

Determination of n is to be done only for one magnet.

Using the data collected also determine the value of magnetic moment M_1 for that magnet.

Take similar data set for the other magnet and determine its magnetic moment M_2.

Calculate the uncertainty in M_1 and M_2.

 Part B: Magnet-magnet interaction

In this part you are going to study the force exerted by one magnet on another magnet along a common axis. One of the magnets is placed on the non-magnetic pan of digital weighing scale. The other magnet is placed in the acrylic tube that can restrict the magnet to move only along its axis as shown in the Figure 9.
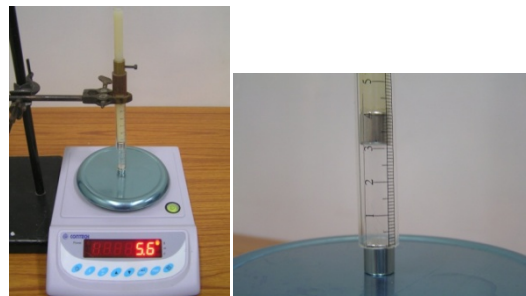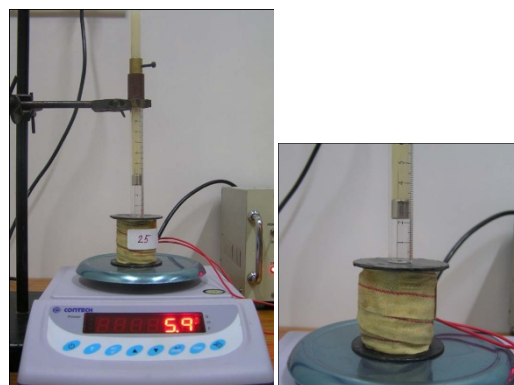

Fig.9 Apparatus arrangement for Part B

When the magnet in the tube repels the magnet on the pan, the normal force on the pan increases. The reading in the pan is a direct measure of the normal force which is proportional to the force of interaction between the magnets. The TARE function in the digital weighing scale can be used appropriately to estimate the force between the magnets. A nylon rod can be used to vary the separation between the magnets. The nylon rod can be adjusted to a desired height by clamping it using the screw provided.

Determine p and K in equation (2) by taking suitable observations and plotting necessary graphs. Justify the rounding of p using uncertainty analysis. Also estimate the uncertainty in K.

Part C: Solenoid – magnet interaction

Fig.10 Apparatus arrangement for Part C

Arrange the apparatus as shown in Figure 10. Before the magnet is inserted in the acrylic tube placed above the solenoid, make sure that there

is some current in the solenoid to make the magnet levitate (Hold the magnet above the solenoid, identify the orientation of the magnet which produces repulsive force). Insert the magnet inside the tube with this orientation.

Determine q and K in equation (3) by taking suitable observations and plotting necessary graphs. For this you may have to vary current in the solenoid and separation between magnet and solenoid.

Area of the solenoid can be calculated using the relation

$$A = \frac{\pi}{3}\left(r_1^2 + r_2^2 + r_1 r_2\right) \tag{6}$$

where r_1 and r_2 are the inner and outer radius of the solenoid.

Plot suitable graphs to determine the q in equation (3). Justify the rounding of value of q using the uncertainty analysis.

Also estimate the uncertainty in K.

Use only magnet 1.

Part D: Determination of relative permeability of soft iron rod.

To determine μ_r from equations (4) and (5) find the value of x for the same currents with and without soft iron rod in the solenoid. Plot a graph to show its variation with current in the solenoid. Use only magnet 1.

Warning:

If the current in the solenoid is less than 0.1 A, then magnet may fall on to the iron core! So keep the current always above 0.1 A.

6. Typical Observations and Calculations

Part A: $V_0 = 4.10$ V

Obs. No.	d /m	V /V	$\Delta V = V - V_0$ /V	B = 0.14 × ΔV /T	ln(d)	ln(B)
1	0.023	4.16	0.06	0.0084	-3.772	-4.780
2	0.022	4.17	0.07	0.0098	-3.817	-4.625
3	0.021	4.18	0.08	0.0112	-3.863	-4.492
4	0.020	4.20	0.10	0.0140	-3.912	-4.269
5	0.019	4.21	0.11	0.0154	-3.963	-4.173
6	0.018	4.23	0.13	0.0182	-4.017	-4.006
7	0.017	4.26	0.16	0.0224	-4.075	-3.799
8	0.016	4.30	0.20	0.0280	-4.135	-3.576
9	0.015	4.32	0.22	0.0308	-4.200	-3.480
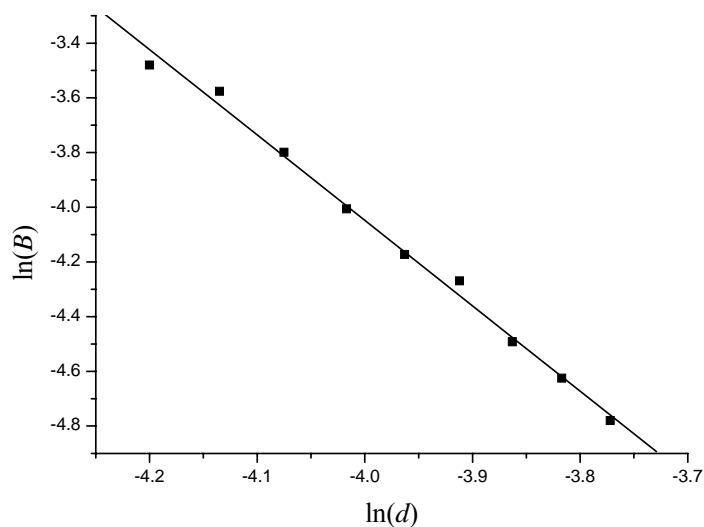
Slope = 3.282

Uncertainty in slope:

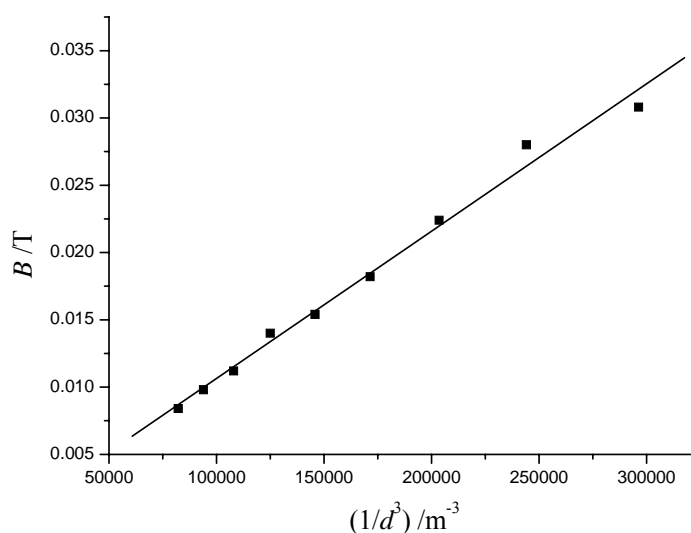$$\frac{\Delta(\text{Slope})}{\text{Slope}} = 0.115$$

$$n = 3.3 \pm 0.4$$

Hence, $n = 3$

For magnet 2:

Obs. No.	d /m	V /V	$\Delta V = V - V_0$ /V	B = 0.14 × ΔV /T
1	0.024	4.16	0.06	0.0084
2	0.023	4.17	0.07	0.0098
3	0.022	4.18	0.08	0.0112
4	0.021	4.19	0.09	0.0126
5	0.020	4.21	0.11	0.0154
6	0.019	4.22	0.12	0.0168
7	0.018	4.24	0.14	0.0196
8	0.017	4.27	0.17	0.0238
9	0.016	4.31	0.21	0.0294

Calculation for determination of magnetic moment of magnet 1 and magnet 2:

Obs. No.	Magnet 1			Magnet 2	
	$\frac{1}{d^3}$ /m^{-3}	B /T		$\frac{1}{d^3}$ /m^{-3}	B /T
1	82190	0.0084		72338	0.0084
2	93914	0.0098		82190	0.0098
3	107980	0.0112		93914	0.0112
4	125000	0.014		107980	0.0126
5	145794	0.0154		125000	0.0154
6	171468	0.0182		145794	0.0168
7	203542	0.0224		171468	0.0196
8	244141	0.028		203542	0.0238
9	296296	0.0308		244141	0.0294

$$\frac{2\mu_0}{4\pi}M_1 = \text{Slope} = 1.188 \times 10^{-7}\,\text{T}\cdot\text{m}^3$$

$$M_1 = \frac{\text{Slope}}{2 \times 10^{-7}} = \frac{1.188 \times 10^{-7}}{2 \times 10^{-7}} = 0.594\,\text{A}\,\text{m}^2$$
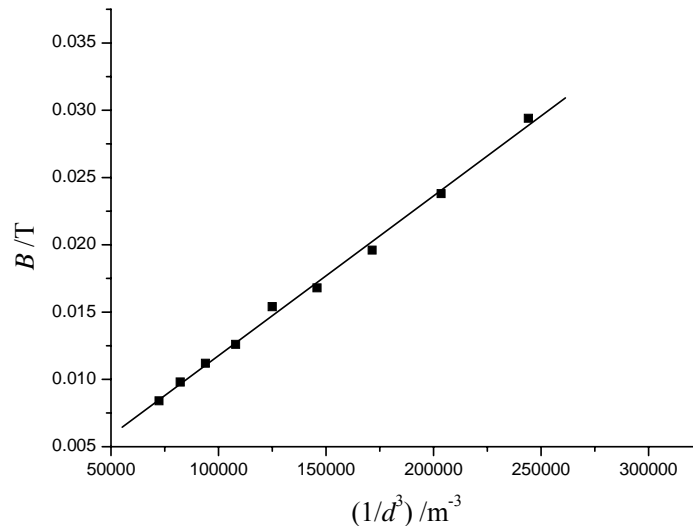
$$\frac{2\mu_0}{4\pi}M_2 = \text{Slope} = 1.089 \times 10^{-7}\,\text{T}\cdot\text{m}^3$$

$$M_2 = \frac{\text{Slope}}{2 \times 10^{-7}} = \frac{1.089 \times 10^{-7}}{2 \times 10^{-7}} = 0.5445\,\text{A}\,\text{m}^2$$

Uncertainty estimation in slope of graph of B Vs $1/d^3$:

Magnet 1:

$$\frac{\Delta M_1}{M_1} = \frac{\Delta(\text{Slope})}{\text{Slope}} = 0.174$$
$$\Delta M_1 = 0.594 \times 0.174 = 0.103\,\text{A}\cdot\text{m}^2$$

Magnet 2:

$$\frac{\Delta M_2}{M_2}\,\frac{\Delta(\text{Slope})}{\text{Slope}} = 0.174$$

$$\Delta M_2 = 0.5445 \times 0.174 = 0.095\,\text{A}\cdot\text{m}^2$$

$$M_1 = 0.594 \pm 0.103 \ \text{A} \cdot \text{m}^2$$

$$M_2 = 0.545 \pm 0.095 \ \text{A} \cdot \text{m}^2$$

Part B:
1) Force as a function of distance:

| Obs. No.	x /m	m /kg	F /N	$\ln(x)$	$\ln(F)$
1	0.021	0.1290	1.2642	-3.863	0.234
2	0.022	0.1085	1.0633	-3.817	0.061
3	0.023	0.0925	0.9065	-3.772	-0.098
4	0.024	0.0753	0.7379	-3.730	-0.304
5	0.025	0.0645	0.6321	-3.689	-0.459
6	0.026	0.0594	0.5821	-3.650	-0.541
7	0.027	0.0482	0.4724	-3.612	-0.750
8	0.028	0.0418	0.4096	-3.576	-0.893
9	0.029	0.0385	0.3773	-3.540	-0.975
10	0.030	0.0340	0.3332	-3.507	-1.099
11	0.031	0.0296	0.2901	-3.474	-1.238
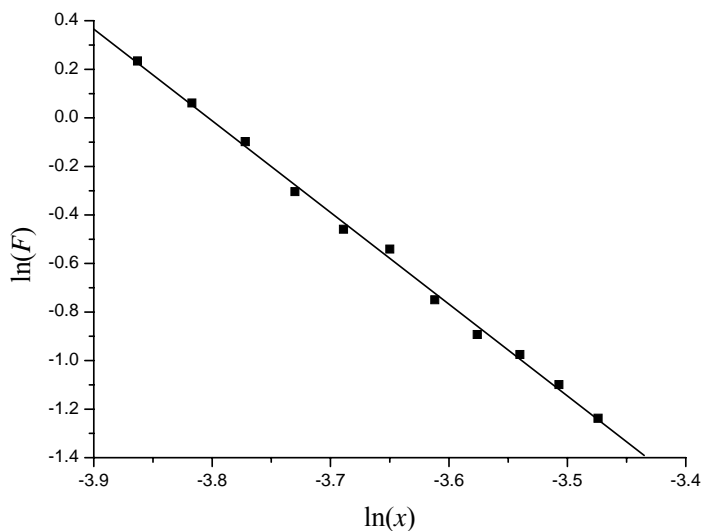
Slope = 4.4

1) Uncertainty estimation in slope of graph of $\ln(F)$ v/s $\ln(x)$

$$\frac{\Delta n}{n} = \frac{\Delta(\text{Slope})}{\text{Slope}} = 0.14$$

$$\Delta n = 0.6$$

$$n = 4.4 \pm 0.6 \approx 4$$

Obs. No.	$(1/x^4)$ /m^{-4}	F /N
1	5.142×10^6	1.2642
2	4.269×10^6	1.0633
3	3.573×10^6	0.9065
4	3.014×10^6	0.7379
5	2.560×10^6	0.6321
6	2.188×10^6	0.5821
7	1.882×10^6	0.4724
8	1.627×10^6	0.4096
9	1.414×10^6	0.3773
10	1.235×10^6	0.3332
11	1.083×10^6	0.2901
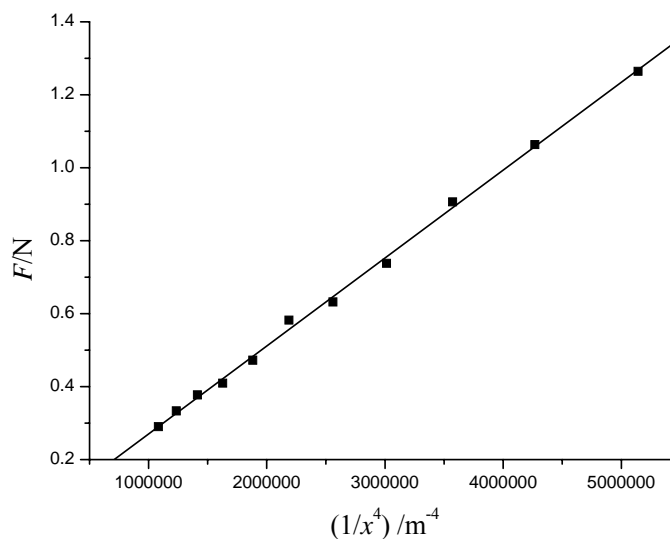
$$K = \frac{Slope}{M_1 M_2} = \frac{2.1995 \times 10^{-7}}{0.594 \times 0.545} = 6.794 \times 10^{-7}\,\text{H m}^{-1}$$

Uncertainty estimation in slope of graph of F Vs $1/x^4$

Magnet 1:

$$\frac{\Delta(\text{Slope})}{\text{Slope}} = 0.157$$

$$\frac{\Delta K}{K} = \sqrt{\left(\frac{\Delta(\text{Slope})}{\text{Slope}}\right)^2 + \left(\frac{\Delta M_1}{M_1}\right)^2 + \left(\frac{\Delta M_2}{M_2}\right)^2} = \sqrt{(0.157)^2 + (0.174)^2 + (0.174)^2} = 0.292$$
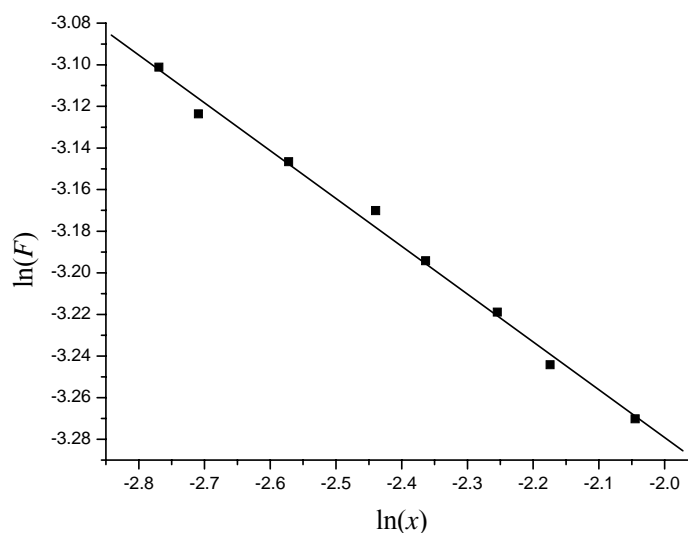
$$\Delta K = 6.794 \times 10^{-7} \times 0.292 = 1.98 \times 10^{-7}\,\text{H} \cdot \text{m}^2$$

Part C:

Solenoid and magnet:
Graph of log (*F*) as function of distance

Obs. No.	x /m	F /N	ln(x)	ln(F)
1	0.045	0.0627	-2.7694	-3.1011
2	0.044	0.0666	-2.7091	-3.1236
3	0.043	0.0764	-2.5718	-3.1466
4	0.042	0.0872	-2.4396	-3.1701
5	0.041	0.0941	-2.3634	-3.1942
6	0.040	0.1049	-2.2547	-3.2189
7	0.039	0.1137	-2.1742	-3.2442
8	0.038	0.1294	-2.0448	-3.2702

Slope = 3.9055

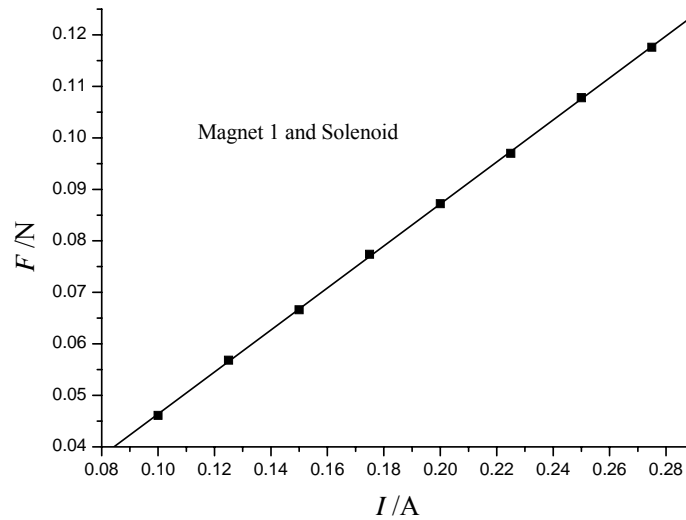1) Uncertainty estimation of graph of ln(*F*) v/s ln(*x*)

$$\frac{\Delta n}{n} = \frac{\Delta(\text{Slope})}{\text{Slope}} = 0.093$$

$$\Delta n = 0.093 \times 3.9055 = 0.36 \approx 0.4$$
$$n = 3.9 \pm 0.4 \approx 4$$

Force versus Current:

Current (A)	Force (N)
0.275	0.1176
0.250	0.1078
0.225	0.0970
0.200	0.0872
0.175	0.0774
0.150	0.0666
0.125	0.0568
0.100	0.0461

Magnet 1 and Solenoid

$$\text{Slope} = 0.42$$

$$K = \frac{\text{Slope} \times x^4}{M \times N \times A} = \frac{0.42 \times 1.87 \times 10^{-6}}{0.594 \times 3000 \times 5.075 \times 10^{-4}} = 8.685 \times 10^{-7} \ \mathrm{H\,m^{-1}}$$

2) Uncertainty estimation of graph F Vs I:

$$\frac{\Delta(\text{Slope})}{\text{Slope}} = 0.066$$

3) Uncertainty in area, A and in x^4:
   Uncertainty in A:

$$\Delta A = \frac{\pi}{3}\left[\left(2 \cdot r_1 \cdot \Delta r_1\right) + \left(2 \cdot r_2 \cdot \Delta r_2\right) + \left(r_1 \cdot \Delta r_2\right) + \left(r_2 \cdot \Delta r_1\right)\right]$$

$\because \Delta r_1 = \Delta r_2$

$$\Delta A = \frac{\pi}{3} \cdot \Delta r_1 \left[3r_1 + 3r_2\right] = \frac{\pi}{3} \times 2 \times 10^{-5} \times \left[\left(3 \times 0.509 \times 10^{-2}\right) + \left(3 \times 1.903 \times 10^{-2}\right)\right] = 1.5147 \times 10^{-6} \ \mathrm{m^2}$$

$$\frac{\Delta A}{A} = \frac{1.5147 \times 10^{-6}}{5.075 \times 10^{-4}} = 2.9846 \times 10^{-3}$$

Uncertainty in x^4:

$$\Delta\left(x^4\right) = 4 \cdot x^3 \cdot \Delta x = 4 \times \left(0.037\right)^3 \times 0.001 = 2.026 \times 10^{-7} \ \mathrm{cm^4}$$

$$\frac{\Delta(x^4)}{x^4} = \frac{2.026 \times 10^{-7}}{1.87 \times 10^{-6}} = 0.1083$$

$$\frac{\Delta K}{K} = \sqrt{\left(\frac{\Delta(\text{Slope})}{\text{Slope}}\right)^2 + \left(\frac{\Delta M_1}{M_1}\right)^2 + \left(\frac{\Delta A}{A}\right)^2 + \left(\frac{\Delta(x^4)}{x^4}\right)^2}$$
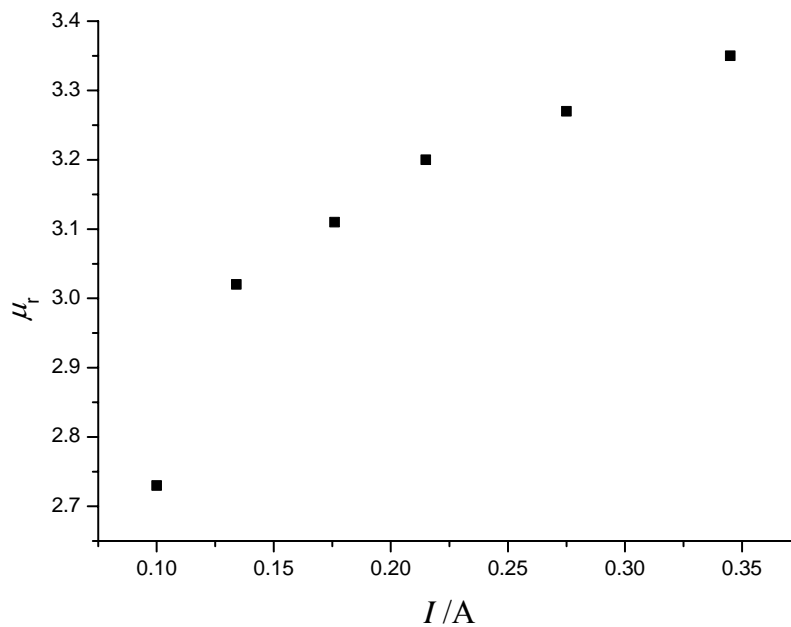
$$\frac{\Delta K}{K} = \sqrt{(0.066)^2 + (0.174)^2 + (0.0029846)^2 + (0.108)^2} = 0.215$$

$$\Delta K = 1.9 \times 10^{-7} \text{ H} \cdot \text{m}^2$$
$$U(K) = 3.8 \times 10^{-7} \approx 4 \times 10^{-7} \text{ H} \cdot \text{m}^2$$

Part D:

Obs. No.	Current, I /A	Air Core Levitation x_a /cm	Iron Core Levitation x_i /cm	$\mu_r = \left(\dfrac{x_i}{x_a}\right)^4$
1	0.100	3.15	4.05	2.73
2	0.127	3.35	4.45	3.11
3	0.134	3.45	4.55	3.02
4	0.176	3.65	4.85	3.11
5	0.215	3.85	5.15	3.20
6	0.275	4.05	5.45	3.27
7	0.345	4.25	5.75	3.35

Conclusion

The magnetic field of the magnet varies as 3rd power of the distance from the magnet. It was also observed that the repulsive force between two cylindrical neodymium magnets is inversely proportional to the 4th power of the distance between the magnets. Similar proportionality was observed for the magnet-solenoid interaction. The experiment also discusses the method to determine the variation of relative permeability of soft iron rod with respect to the current through solenoid.

Acknowledgements

Physics Through Problem Solving XXV: Small Oscillations

Ahmed Sayeed

Department of Physics

University of Pune

Pune - 411007

email: sayeed@physics.unipune.ac.in

Abstract

In this issue we solve some problems on small oscillations.

When a system of particles is disturbed slightly from its equilibrium configuration momentarily and released, it will undergo oscillations about the equilibrium configuration. These oscillations in general can be nonlinear and very complicated and very difficult to analyze. But there is one special category of oscillations where the problem simplifies greatly – and this is the category of 'small oscillations'. If a collection of mutually interacting particles oscillate in such a way that the forces acting on them can be well approximated by Hooke's law forces, they can be considered small oscillations. It so happens that any restoring force can be approximated by a Hooke's law force if the displacement of the particle from the equilibrium position (i.e., the position where the restoring force is zero) is small enough. For a full discussion of the nature of small oscillations the reader should refer any of the standard classical mechanics texts, such as the ones by Goldstein, Poole & Safko [2] or by Rana & Joag [1].

The first two problems below are short, and are meant to illustrate how some arbitrary restoring force acting on a single particle is approximated by a Hooke's law force. The third is a longer problem with two particles, which is meant to illustrate the general method of solving the motion of coupled oscillators. In this issue we will only find the normal frequencies for a system of coupled oscillators. In a future issue we shall consider the problem of finding the amplitudes in terms of normal modes.

Problem 1

Consider the Lennard-Jones Potential, which is used as an approximate model for the potential energy of interaction between two neutral atoms or molecules:

$$V(r) = 4\epsilon \left[\left(\frac{\sigma}{r}\right)^{12} - \left(\frac{\sigma}{r}\right)^{6} \right] \qquad (1)$$

where r is the separation between the two atoms or molecules, and $\epsilon > 0$ and $\sigma > 0$ are constants. For an atom or molecule moving under this potential, find the frequency of small oscillations about the position of stable equilibrium.

Solution

What we are going to do here is to find an approximate expression of the form $\frac{1}{2}kr^2$ for the potential energy $V(r)$ ($k > 0$ is the spring constant), so that the resulting force is the Hooke's law force $F = -kr$, and the motion is simple harmonic with the frequency $w = \sqrt{k/m}$, where m is the mass of the particle.

At stable equilibrium position $r = r_0$ the potential energy given by eq. 1 is a minimum, which means

$$\left(\frac{\partial V}{\partial r}\right)_{r=r_0} = 0$$

$$\implies 4\epsilon \left(-\frac{12\sigma^{12}}{r^{13}} + \frac{6\sigma^6}{r^7}\right)_{r=r_0} = 0$$

$$\implies 4\epsilon \left(-\frac{12\sigma^{12}}{r_0^{13}} + \frac{6\sigma^6}{r_0^7}\right) = 0$$

$$\implies r_0 = 2^{1/6}\sigma \qquad (2)$$

The spring constant for small oscillations is given by

$$k = \left(\frac{\partial^2 V}{\partial r^2}\right)_{r=r_0}$$

$$= 4\epsilon \left(-\frac{12\sigma^{12}}{r_0^{13}} + \frac{6\sigma^6}{r_0^7}\right)$$

Substituting for r_0 from eq.2 and simplifying we get

$$k = \frac{72\epsilon}{2^{1/3}\sigma^2} \qquad (3)$$

Note that $k > 0$, as it should be, because it is the value of the second derivative of $V(r)$ at the minimum. And also we require the spring constant to be positive. The frequency of small oscillations is

$$\omega = \sqrt{\frac{k}{m}} = \sqrt{\frac{72\epsilon}{2^{1/3}\sigma^2 m}}$$

where m is the mass of the particle.

Problem 2

The following potential, know as Morse potential is sometimes used as an approximate model for the potential energy of interaction between atoms in a diatomic molecule:

$$V(r) = D \left(1 - e^{-\alpha(r-a)}\right)^2 \qquad (4)$$

where r is the separation between the two atoms, and $D > 0$, $\alpha > 0$, and $a > 0$ are constants. For an atom moving under this potential, find the frequency of small oscillations about the position of the stable equilibrium.

Solution

Once again we first find the equilibrium position $r = r_0$, which is the minimum position for the potential energy $V(r)$ of eq. 4.

$$\left(\frac{\partial V}{\partial r}\right)_{r=r_0} = 0$$

$$\implies 2D\alpha \left((r-a)e^{-\alpha(r-a)^2} \right)_{r=r_0} = 0$$

$$\implies 2D\alpha(r_0-a)e^{-\alpha(r_0-a)^2} = 0$$

$$\implies r_0 = a \qquad (5)$$

The last equation follows by noting that $e^{-\alpha(r-a)^2}$ is never zero for finite r and therefore $(r_0 - a) = 0$. And the spring constant is

$$
\begin{aligned}
k &= \left(\frac{\partial^2 V}{\partial r^2} \right)_{r=a} \\
&= 2D\alpha \left(e^{-\alpha(r-a)^2} + 2\alpha(r-a)^2 e^{-\alpha(r-a)^2} \right)_{r=a} \\
&= 2D\alpha \qquad\qquad (6)
\end{aligned}
$$

Once again k is positive, as it must be. The frequency of small oscillations on the equilibrium position, for a particle of mass m is

$$\omega = \sqrt{\frac{k}{m}} = \sqrt{\frac{2D\alpha}{m}}$$

Problem 3

Find the normal frequencies of oscillations for a double pendulum undergoing small oscillations in a single vertical plane. Consider the special case of equal masses and the lengths.

Solution Let me briefly describe what are 'normal frequencies'. In a system of couple oscillators, even when the oscillations are small and the forces can be approximated by Hooke's law forces, the general motion is not simple harmonic or even periodical. But it can always be represented as a superposition of simple harmonic motions. The frequencies of these simple harmonic motion are called
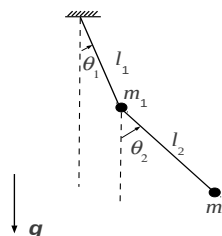

Figure 1: A double pendulum. See the text for description.

normal frequencies. It is possible for the system to oscillate in such a way that all of the particles undergo simple harmonic motions with a single frequency, which is one of the normal frequencies. Such a motion is called a normal mode. In following we shall find the normal frequencies for the double pendulum and we shall find the corresponding normal

modes in another issue.

The figure 1 shows the the double pendulum – where m_1, m_2 are the masses, l_1, l_2 are the two string lengths, and θ_1, θ_2 are the two angular displacements from the equilibrium position, which is $\theta_1 = \theta_2 = 0$. **g** is the acceleration due to gravity. This is a system with two degrees of freedom, and we can use θ_1, θ_2 as our generalized coordinates. Note that for the analysis of small oscillations it is convenient if we choose generalized coordinates such that they take values zero at the equilibrium position, and that is what we have done here. Finding the potential and kinetic energies in generalized coordinates for a double pendulum is a very routine exercise in classical mechanics courses, and so we omit the details and directly write down the expressions. We hope the reader can easily verify them. Taking the potential energy as zero at $\theta_1 = \theta_2 = 0$. **g**, we get

$$V(\theta_1, \theta_2) = -m_1 g l_1 \cos\theta_1 - m_2 g(l_1 \cos\theta_1 + l_2 \cos\theta_2) \tag{7}$$

$$T(\theta_1, \theta_2, \dot{\theta}_1, \dot{\theta}_2) = \frac{1}{2}m_1 l_1^2 \dot{\theta}_1^{\,2} + \frac{1}{2}m_2 \left[l_1^2 \dot{\theta}_1^{\,2} + l_2^2 \dot{\theta}_2^{\,2} + 2 l_1 l_2 \dot{\theta}_1 \dot{\theta}_2 \cos(\theta_1 - \theta_2) \right] \tag{8}$$

The above expressions 7 and 8 for the potential and the kinetic energies of the system are valid for all value of generalized positions θ_1, θ_2 and the generalized velocities $\dot{\theta}_1, \dot{\theta}_2$. But we need to approximate these expressions for small values of the positions and velocities. These expressions take the following form:

$$V = \frac{1}{2} \sum_i \sum_j V_{ij} \theta_i \theta_j \tag{9}$$

$$T = \frac{1}{2} \sum_i \sum_j T_{ij} \dot{\theta}_i \dot{\theta}_j \tag{10}$$

where $i, j = 1, 2$, and the coefficients V_{ij} and T_{ij} are constants (i.e, not functions of coordinates or velocities) to be determined. In the case of potential energy these coefficient are nothing but the Taylor series expansion coefficients about the equilibrium position (compare with the problems 1 and 2 above). Thus V_{11} is the coefficient of the first non-vanishing term in the Taylor series expansion in the variable θ_1:

$$
\begin{aligned}
V_{11} &= \left(\frac{\partial^2 V}{\partial \theta_1^2} \right)_{\theta_1 = 0} \\
&= (m_1 g l_1 \cos\theta_1 + m_2 g l_1 \cos\theta_1)_{\theta_1 = 0} \\
&= (m_1 + m_2) g l_1
\end{aligned}
$$

Similarly

$$
\begin{aligned}
V_{12} &= \left(\frac{\partial^2 V}{\partial \theta_1 \partial \theta_2} \right)_{\theta_1 = \theta_2 = 0} \\
&= 0 \\
V_{21} &= V_{12} = 0
\end{aligned}
$$

$$V_{22} = \left(\frac{\partial^2 V}{\partial \theta_2^2}\right)_{\theta_2=0}$$
$$= m_2 g l_2$$

Thus the potential energy of eq. 9 is

$$V = \frac{1}{2}\left[(m_1 + m_2)gl_1\theta_1^2 + m_2gl_2\theta_2^2\right] \quad (11)$$

We do a similar exercise to the kinetic energy in the form of eq. 10. The idea is to

take the Taylor series expansion of the kinetic energy given in eq. 8 such that only the terms quadratic in velocities (i.e, the terms $\dot{\theta_1}^2, \dot{\theta_2}^2, \dot{\theta_1}\dot{\theta_2}$) are retained. We can see that eq. 8 is already in that form, except for the factor $\cos(\theta_1 - \theta_2)$ in the last term. Therefore we expand this factor in Taylor series and retain the first non-zero term, which is 1. Thus, the kinetic energy in eq. 10 is given by

$$T(\dot{\theta_1}, \dot{\theta_2}) = \frac{1}{2}m_1l_1^2\dot{\theta_1}^2 + \frac{1}{2}m_2\left[l_1^2\dot{\theta_1}^2 + l_2^2\dot{\theta_2}^2 + 2\dot{\theta_1}\dot{\theta_2}l_1l_2\right]$$
$$= \frac{1}{2}\left[(m_1 + m_2)l_1^2\dot{\theta_1}^2 + m_2l_2^2\dot{\theta_2}^2 + 2m_2l_1l_2\dot{\theta_1}\dot{\theta_2}\right] \quad (12)$$

And thus $T_{11} = (m_1 + m_2)l_1^2, T_{12} = T_{21} = m_2l_1l_2, T_{22} = m_2l_2^2$ (You have to note that $2m_2l_1l_2\dot{\theta_1}\dot{\theta_2} = m_2l_1l_2\dot{\theta_1}\dot{\theta_2} + m_2l_1l_2\dot{\theta_2}\dot{\theta_1}$ to correctly compare eqs. 10 and 12 and identify T_{12} and T_{21}).

Thus eqs. 11 and 12 give us the two matrices:

$$\mathbb{V} = \begin{bmatrix} V_{11} & V_{12} \\ V_{21} & V_{22} \end{bmatrix}$$
$$= \begin{bmatrix} (m_1 + m_2)gl_1 & 0 \\ 0 & m_2gl_2 \end{bmatrix} \quad (13)$$

and

$$\mathbb{T} = \begin{bmatrix} T_{11} & T_{12} \\ T_{21} & T_{22} \end{bmatrix}$$
$$= \begin{bmatrix} (m_1 + m_2)l_1^2 & m_2l_1l_2 \\ m_2l_1l_2 & m_2l_2^2 \end{bmatrix} \quad (14)$$

At this point we consider the special case of equal masses and lengths, i.e. $m_1 = m_2 = m$ and $l_1 = l_2 = l$. Then the two matrices simplify to

$$\mathbb{V} = \begin{bmatrix} 2mgl & 0 \\ 0 & mgl \end{bmatrix} \quad (15)$$

And

$$\mathbb{T} = \begin{bmatrix} 2ml^2 & ml^2 \\ ml^2 & ml^2 \end{bmatrix} \quad (16)$$

The normal frequencies ω are given by the solutions to the equation

$$det\left(\mathbb{V} - \omega^2\mathbb{T}\right) = 0$$
$$det\begin{bmatrix} 2mgl - 2ml^2\omega^2 & -ml^2\omega^2 \\ -ml^2\omega^2 & mgl - ml^2\omega^2 \end{bmatrix} = 0$$

We can simplify the above equation substituting $g = l\omega_0^2$, and canceling out ml^2 throughout (also note that $\omega_0 = \sqrt{g/l}$ happens to be the frequency of a simple pendulum of length l), to get

$$det \begin{bmatrix} 2(\omega_0^2 - \omega^2) & -\omega^2 \\ -\omega^2 & (\omega_0^2 - \omega^2) \end{bmatrix} = 0$$

Expanding the determinant and simplifying we get

$$\omega^4 - 4\omega_0^2\omega^2 + 2\omega_0^4 = 0$$

which is a quadratic equation in ω^2 and has two solutions

$$\omega_1^2 = (2 + \sqrt{2})\omega_0^2$$

$$\omega_2^2 = (2 - \sqrt{2})\omega_0^2$$

Thus ω_1 and ω_2 are the normal frequencies.

References

[1] N C Rana and P S Joag (1991). Classical Mechanics, Tata McGraw Hill, New Delhi

[2] H Goldstein & C P Poole and J Safko Classical Mechanics, Pearson, New Delhi

News: Nobel Prize in Physics 2012

honours

Serge Heroche and David J Wineland

Abstract

Nobel Prize for 2012 celebrates the "ground-breaking experimental methods that enable measurement and manipulation of individual quantum systems" and goes to **Serge Haroche**, Collège de France, Paris, France, École Normale Supérieure, Paris, France and **David J. Wineland**, National Institute of Standards and Technology, Boulder, CO, USA, University of Colorado, Boulder, CO, USA.

This year's Nobel Prize in Physics celebrates the triumph of experimental methods in isolating and manipulating individual quantum systems. A quantum system is described by a wavefunction and the measurement outcome is always statistical. Measurement process often alters the state, so much so that the state is destroyed by trying to measure it.

Serge Haroche and David Wineland succeeded in making direct observation of individual quantum systems, such as a single atom and a single photon trapped in a suitable cavity long enough to observe *directly* the quantum attributes without destroying the state.

Both Laureates worked in the field of Quantum Optics with complementary techniques: David Wineland trapped electrically charged ions in a cavity made with with electric field configurations and studied their interaction with light (photon) and Serge Haroche did the opposite. He trapped photons with a set of mirrors and let them interact by sending (Rydburg) atoms through the trap.

In Heroche's lab the microwave photons are trapped in a cavity made up of superconducting mirrors so that a single photon bounces about for as long as a second. This is long enough to prepare the photon in an entangled state (a superposed state of photon) of its polarisation. This state is viewed with the help of Rydburg atoms (specially prepared atomic states that are nearly 1000 times the size of usual atoms) sent individually into the cavity. The phase of the exiting Rydburg atoms signals the presence of entangled photon in the cavity without being destroyed by the measurement.
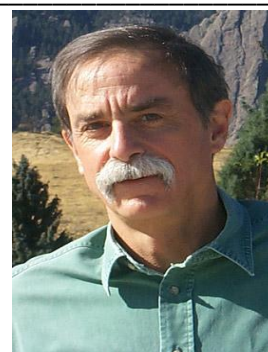
In Wineland's experiment the atomic state of the trapped ion could be manipulated to be in a superposed state, say of two different energy eigenstates, achieved by gently nudging by a photon of intermediate frequency - a clear demonstration of Quantum Mechanics in action.

While on the one hand these experiments confirm the corner stone of Quantum Mechanics, they also pave way to their application in many scenes, such as making ultra precise clocks, getting to the next step in achieving a Quantum Computer etc.

R Ramachandran
Physics Education

Serge Heroche

David J Wineland